



저작자표시-비영리-변경금지 2.0 대한민국

이용자는 아래의 조건을 따르는 경우에 한하여 자유롭게

- 이 저작물을 복제, 배포, 전송, 전시, 공연 및 방송할 수 있습니다.

다음과 같은 조건을 따라야 합니다:



저작자표시. 귀하는 원저작자를 표시하여야 합니다.



비영리. 귀하는 이 저작물을 영리 목적으로 이용할 수 없습니다.



변경금지. 귀하는 이 저작물을 개작, 변형 또는 가공할 수 없습니다.

- 귀하는, 이 저작물의 재이용이나 배포의 경우, 이 저작물에 적용된 이용허락조건을 명확하게 나타내어야 합니다.
- 저작권자로부터 별도의 허가를 받으면 이러한 조건들은 적용되지 않습니다.

저작권법에 따른 이용자의 권리는 위의 내용에 의하여 영향을 받지 않습니다.

이것은 [이용허락규약\(Legal Code\)](#)을 이해하기 쉽게 요약한 것입니다.

[Disclaimer](#)

# **Analysis of Relative Humidity Effects on Ejector Performance**

**Hochae Lee**

**School of Mechanical Engineering**

**Seoul National University, Seoul, Korea**

## **Abstract**

**Pumping in ejectors is a measure of how much the secondary fluid is entrained by the high momentum primary flow and is one of the crucial performance indices. In the fuel recirculation system of fuel cells, the entrained secondary fluid contains water vapor due to the over-supplied hydrogen, making the secondary fluid humid. In such cases, the relative humidity of the secondary fluid alters the fluid properties of the mixed flow. This study examines such effects of relative humidity on ejector. A new analytical model has been**

developed, and series of measurements has been conducted to validate the model's prediction. The present results demonstrate that higher relative humidity of the secondary fluid reduces pumping in an ejector. During the mixing process of the two fluids, condensation releases heat, increasing the ejector operating temperature. Thus, secondary flow density is decreased, and pumping is lowered.

**Keywords: Ejector performance, Relative humidity, Condensation, Fuel cell automobile**

**Student number: 2007-20844**

# Contents

<b>Abstract</b> .....	i
<b>Contents</b> .....	iii
<b>List of figures</b> .....	v
<b>List of tables</b> .....	viii
<b>Nomenclatures</b> .....	ix
<b>Chapter 1. Introduction</b> .....	1
1.1 Background and motivation .....	1
1.2 Research objectives .....	7
1.3 Approach and scope .....	8
1.4 Thesis organization.....	9
<b>Chapter 2. One-dimensional Analysis of an Ejector</b> .....	10
2.1 Introduction.....	10
2.1.1 Condensation effect.....	15
2.1.2 Change of thermo-physical properties of humid air....	17
2.2 Modeling procedure.....	22
2.3 Conclusions.....	29

<b>Chapter 3. Measurement of Pumping Degradation due to Humidity</b> .....	31
3.1 Introduction.....	31
3.2 Experiment of an ejector with humid secondary flow.....	33
3.2.1 Experiment setup.....	33
3.2.2 Ejector Design.....	50
3.2.3 Uncertainty analysis.....	63
3.3 Test result.....	65
3.4 Conclusions .....	71
<b>Chapter 4. Modelling Result and Discussion</b> .....	72
4.1 Ejector pumping and condensation.....	72
4.2 Effect of secondary temperature on ejector performance.....	76
4.3 Effect of pressure drop due to condensation.....	81
4.4 Variation of thermos-physical properties.....	83
4.5 Ejector characteristics.....	86
4.6 Conclusions .....	90
<b>Chapter 5. Summary and conclusions</b> .....	92
<b>References</b> .....	95
<b>Abstract (Korean)</b> .....	100

# List of Figures

Fig. 1.1. Typical ejector geometry

Fig. 1.2. An ejector refrigeration system [29].

Fig. 1.3. IRS ejector installed in a helicopter. (Courtesy of US Army)

Fig. 1.4. Example of fuel recirculation system in PEMFC [11].

Fig. 2.1. Major geometries of an ejector.

Fig. 2.2. Dew point of secondary flow (330K) vs. primary flow temperature. (300K)

Fig. 2.3. Humidity and temperature effect on density.

Fig. 2.4. Humidity and temperature effect on specific heat capacity.

Fig. 2.5. Humidity and temperature effect on specific heat ratio.

Fig. 2.6. Control volume of analysis.

Fig. 2.7. Analysis flow chart.

Fig. 3.1. Schematic of the experiment setup.

Fig. 3.2. Photo of the experiment setup.

Fig. 3.3. Photo of the test ejector.

Fig. 3.4. Compressed air tanks.

Fig. 3.5. Pressure chamber.

Fig. 3.6. Mass flow rate meter used in primary flow (GR112-1-A-PO).

Fig. 3.7. Mass flow rate meter used in secondary flow (GR112-1-A-PO).

Fig. 3.8. Pressure sensor used in primary and exit flow (FPA).

Fig. 3.9. Pressure sensor used in secondary flow (BARATRON 698A13TRA).

Fig. 3.10. Schematic of the humidifier.

Fig. 3.11. Photo of the humidifier.

Fig. 3.12. Two types of an ejector nozzle. (a) subsonic nozzle, (b) supersonic nozzle.

Fig. 3.13. Two types of an ejector mixing tube. (a) constant area mixing, (b) constant pressure mixing

Fig. 3.14. Three-dimensional view of the designed ejector.

Fig. 3.15. Primary nozzle.

Fig. 3.16. Nozzle holder.

Fig. 3.17. Mixing chamber sealing.

Fig. 3.18. Mixing chamber.

Fig. 3.19. Secondary flow inlet

Fig. 3.20. Measured pumping of secondary flow vs. relative humidity.

Fig. 3.21. Condensed water at the ejector exit.

Fig. 4.1. Pumping of secondary flow vs. relative humidity.

Fig. 4.2. Comparison of new model vs. Greitzer model.

Fig. 4.3. Pumping with temperature variation ( $\theta=1.06, 1.10, 1.14$ ).

Fig. 4.4. Condensed vapor with temperature variation

( $\theta=1.06, 1.10, 1.14$ ).

Fig. 4.5. Thrust augmentation with temperature variation

( $\theta=1.06, 1.10, 1.14$ ).

Fig. 4.6. Pumping degradation with pressure drop due to condensation.

Fig. 4.7. Density variation vs. relative humidity for  $\theta = 1.06, 1.10$ , and 1.14: (a) with condensation and (b) without condensation

Fig. 4.8. Specific heat ratio variation vs. relative humidity for  $\theta = 1.06, 1.10$ , and 1.14: (a) with condensation and (b) without condensation

Fig. 4.9. Performance map of the ejector.

Fig. 4.10. Operational modes of an ejector.



## List of tables

Table 3.1. List of sensors used in experiment setup.

Table 3.2. Specification of the humidifier.

Table 3.3. Part descriptions of the humidifier.

Table 3.4. Designed ejector.

Table 3.5. Experiment result at design point for zero relative humidity

Table 3.6. Experiment data using humid secondary flow.

# Nomenclatures

$a$	Speed of sound
$D$	Diameter
$c_p$	Specific heat capacity, constant pressure
$c_v$	Specific heat capacity, constant volume
$F$	Faraday constant
$h$	Enthalpy
$h_{fg}$	Latent heat
$I$	Stack load
$k$	Specific heat ratio
$M$	Molar mass
$\dot{m}$	Mass flow rate
$N$	Amount of single cells
$P$	Pressure
$P_{sv}$	Saturated vapor pressure
$R$	Gas constant

$r$	Radius
$T$	Temperature
$T_{\text{sat}}$	Saturation temperature
$U$	Uncertainty
$u$	Velocity
$\dot{V}$	Volumetric flow rate

#### Greek

$\eta$	Ejector efficiency
$\theta$	Primary to secondary temperature ratio
$\lambda$	Stoichiometric ratio
$\Pi$	Pressure ratio
$\rho$	Density
$\Phi$	Pumping (divided by design point pumping)
$\phi$	Pumping (divided by primary flow)

## Abbreviations

AH Absolute humidity

RH Relative humidity

## Non-dimensional parameter

Ja Jakob number

Ma Mach number

## Subscripts

a Air

atm Standard atmospheric condition

e Exit

p Primary

s Secondary

t Total

s Static

v Vapor



# Chapter 1.

## Introduction

### 1.1 Background and motivation

An ejector is a pump without moving parts and is composed of a stationary nozzle for the primary high momentum fluid flow and a mixing tube. Fig. 1.1 shows typical ejector geometry. The primary flow is ejected from the nozzle, entraining the secondary fluid surrounding the primary nozzle, and the two streams are mixed in the mixing tube. Due to their simplicity, ejectors have been widely used in various applications, including refrigeration, air-conditioning, and aircraft systems.

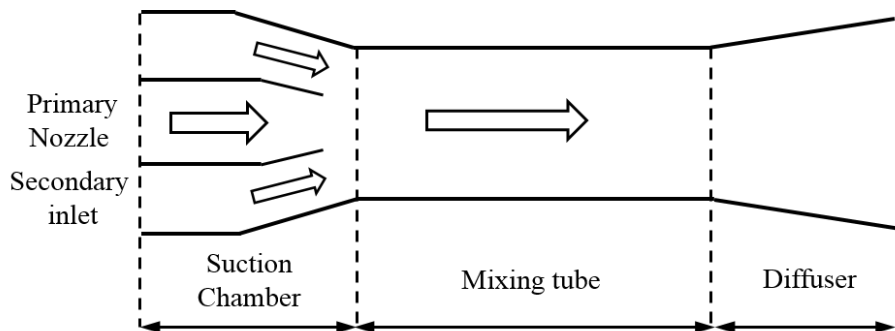


Fig. 1.1. Typical ejector geometry

Many aspects of ejectors have been a subject of studies over the years. Keenan and Neumann [1] and Keenan et al. [2] proposed 1-D analytical ejector models and provided experimental validation. Their models assumed inviscid, isentropic processes and were based on the conservation laws (mass, momentum and energy). Elrod [3] suggested an analytical model to obtain the optimal area ratio for pumping. Eames et al. [4] and Huang et al. [5] extended Keenan's 1-D approach by including frictional losses and predicted ejector performance for various geometries. Presz and Greitzer [6] used control volume analysis to show that ejector pumping performance depends on the area and temperature ratios.

Sheriff et al. [7] derived an isentropic homogeneous model for two-phase flow ejectors. In this model, the primary fluid was a two-phase mixture and the secondary fluid was either a sub-cooled or saturated liquid. Their model predicted ejector performance by accounting for phase transformation due to compression, expansion, and mixing processes. However, their model did not consider changes in the fluid properties during mixing. Cizungu et al. [8] derived a thermodynamic model of two-phase ejectors using control volume analysis. They used a mixture of  $\text{NH}_3$  and  $\text{H}_2\text{O}$  for modeling, and the model assumed a homogeneous working fluid.

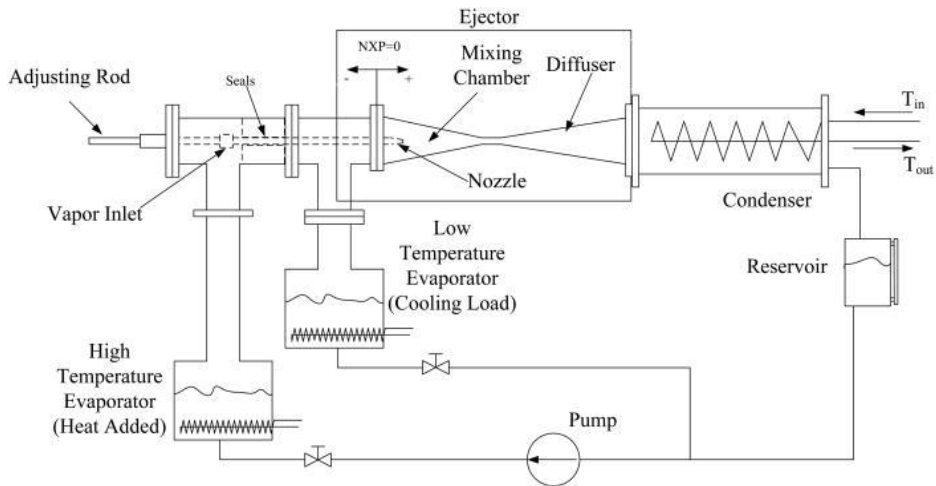


Fig. 1.2. An ejector refrigeration system [29].

Ejectors operating in humid condition can be found commonly. For example, air-conditioning system that uses ejector as a pump can be operated in humid working fluid due to condensation. Elbel [6] summarized present applications in air-conditioning and refrigeration and importance of an ejectors in those systems. In air-conditioning system, control of temperature and humidity for human comfort is important. Also, humidity control in air-conditioning is important in museum and library. Shirey [7] demonstrated humidity control in art museum using heat exchanger containing an ejector with controls of air conditioning system. ASHRAE [8] stated that systems with ejector are extensively used in applications of drying medicines and food items. In aerospace applications, weather condition can vary the humidity of



primary or secondary flow depending on the purpose of ejector. For example, an ejector used in IRS (Infrared Suppression) system entrains ambient air as a secondary flow. Depending on weather conditions, humidity can impact of performance of an ejector. Helicopter's overall system including infrared signature reduction system also faces varying humidity due to weather conditions. FAA [9] recommend to operate helicopter with higher caution in hot, humid condition because it requires more power than operating in dry conditions.



Fig. 1.3. IRS ejector installed in a helicopter. (Courtesy of US Army)

In fuel cell stacks, a fuel recirculation ejector entrains a mixture of unreacted hydrogen and vapor while primary flow supplies pure hydrogen.

The vapor is a product of the electrochemical reaction, and it makes secondary flow humid. Marsano et al. [9] designed and analyzed a solid oxide fuel cell (SOFC) recirculation ejector performance and off-design behavior. However, their model assumed perfectly dry hydrogen supply. Kim et al. [10] designed and tested a fuel recirculation ejector as part of submarine proton exchange membrane fuel cell (PEMFC) system. Their design procedure assumed a homogeneous mixture of hydrogen and water vapor as the working fluid and did not consider condensation. Zhu and Li [11] developed a 2-D model for an ejector used in a PEMFC system which included a humidifier installed at the ejector exit. However, their model did not consider humidity change in the system. Engelbracht et al. [12] modeled and compared a fuel-driven ejector and steam-driven ejector for an SOFC fuel recirculation system, and they described the working fluid in terms of fuel utilization ratio rather than relative humidity.

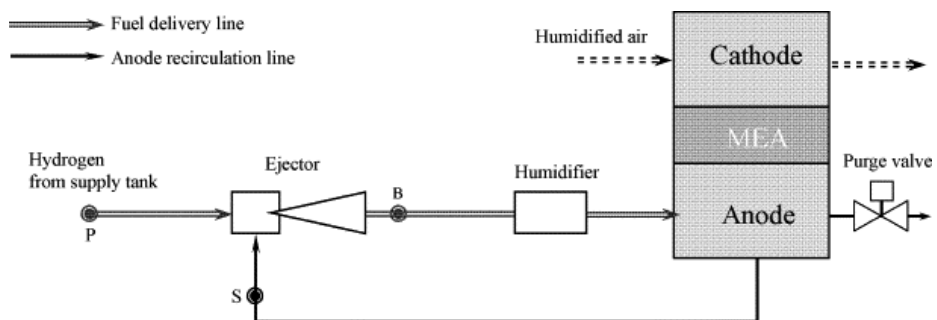


Fig. 1.4. Example of fuel recirculation system in PEMFC [11].

Despite of many researches, there are still unknown factors that affects ejector performance. Factors that affect ejector performance can be classified into two; geometric configuration and flow condition. In this study, effect of humidity which changes a flow condition will be discussed. Although relative humidity can affect ejector performance since it changes flow properties, ejectors using humid air as a primary working fluid have not been researched. Humid air has different properties and behavior compared to a mixture of two gases. Ignoring humidity can lead to significant error due to the relatively low molar mass of water vapor, and such effect is amplified at higher humidity. Therefore, the objectives of this study are to measure and analyze the impact of relative humidity on the ejector pumping. Specific questions to investigated are as follows:

- i) How does relative humidity affect ejector pumping?
- ii) What is the mechanism that affects pumping in a humid ejector?

## 1.2 Research objectives

Research objectives of this study are as follows:

- i) Build analytical model of “humid” ejector to predict performance.
- ii) Measure pumping of ejector with humid secondary flow.

Specific questions to investigated are as follows:

- 1) How does relative humidity affect ejector performance?
- 2) What is the mechanism that affects performance in a “humid” ejector?

### **1.3 Approach and scope**

New ejector model is developed to investigate the effect of humidity on ejector performance analytically. This model uses one-dimensional control volume analysis, correlation of humid air's properties and condensation effect. The new model predicts effect of a relative humidity on an ejector pumping and its characteristic map.

To validate the new model an experiment was conducted. An ejector has been designed and tested using humidifier installed at secondary flow inlet. An ejector performance such as pumping performance has been measured by varying a relative humidity of secondary flow.

## 1.4 Thesis organization

This thesis consists of three chapters. The individual description of chapters are as follows.

Chapter 1 introduces the importance of a relative humidity on the ejector performance. Previous studies are reviewed and the motivation and objectives are presented.

Chapter 2 presents the new analytical model for an ejector using humid working fluid.

Chapter 3 presents design and experiment of an ejector using humid secondary flow to verify the analytical model presented in chapter 2.

Chapter 4 presents the model's prediction and compare with experiment results. Also, discussion on the ejector performance is presented.

Chapter 5 summarizes the results and presents conclusions.

## Chapter 2.

### One-dimensional Analysis of an Ejector

#### 2.1 Introduction

Major factors affecting the ejector performance can be classified into two: geometric configurations and flow conditions. Mainly studied geometry effect is an area ratio of the primary and secondary nozzle, shape of the nozzle, a mixing tube length, position of the primary nozzle and eccentricity of nozzle and mixing tube. Effect of the area ratio was studied extensively since it is a key factor determining pumping of the ejector. [1-5] As area ratio increases, pumping of the ejector also increases. Effect of the nozzle shape is another factor affecting the ejector performance. It is primarily used to increase mixing inside the ejector, thus increasing pumping performance. Carletti et al. [25] tested two different nozzles, one having vortex generator inside a primary nozzle and the other without vortex generator. Both nozzle was a round shaped. Their experiment showed that having vortex generator increases an ejector pumping by up to 40%. McBean et al. [26] installed tabs at the exit of the primary nozzle and varied the number of tabs and the angle

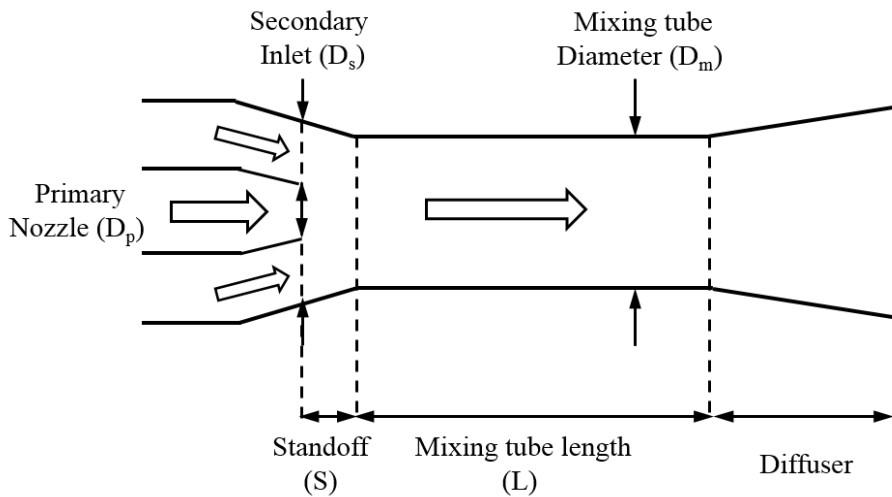


Fig. 2.1. Major geometries of an ejector.

between the tab and a nozzle. They reported increment of mass entrainment up to 20% compared to plain nozzle. They also observed that vortex generated by tabs increases mixing layer, increasing pumping performance. Effect of the mixing tube length was studied by Im et al. [27]. They varied length of the mixing tube from two to four times of the mixing tube diameter. their experiment and analytical model explained the phenomena using jet expansion theory. Due to the short mixing tube, primary and secondary flow does not fully mix. Decreased mixing performance of the ejector directly reduces pumping. Another key geometry of an ejector is axial standoff which is defined as a distance between a primary nozzle and a mixing tube. Experiments done by



various researchers suggest standoff distance to primary nozzle diameter ratio of 2. Carletti et al. [25] and McBean et al. [26] tested ejectors by varying axial standoff distance. As standoff increases from 0 to 2, pumping of the ejector also increased. However, analytical model to describe the effect of axial standoff has not been developed.

Flow conditions are other major factor that affects performance of an ejector. Temperature ratio of secondary to primary flow has been investigated by various researchers [1-5]. One of the findings shows that as temperature of secondary flow increases, pumping performance of the ejector also increases [16]. Another topic of interest is selection of working fluid. In refrigeration applications, various refrigerants such as R134a is used. Refrigerants have different thermos-physical properties compared to air or water. Also, when operating an ejector refrigeration system, a working fluid can be either dry vapor or wet vapor depending on operating condition. Operating in a wet fluid condition, small droplets may block the effective area of an ejector hence, deteriorating overall performance [28].

Analytical models to represent such ejectors has been developed either single phase or two phase model. One-dimensional single phase model has been suggested by Keenan et al. [2]. However, their model

cannot predict choking phenomenon which is common operation mode of an ejector. To overcome the limitation of Keenan's model, Eames et al. [4] and Huang et al. [5] developed one-dimensional model based on two streams mixing model. All of above models assumed a working fluid as ideal gas which have limitation predicting actual process inside an ejector.

To overcome shortage of single phase models, some researchers approached an ejector flow as two phase model. Sherif et al. [10] derived isentropic homogenous model to represent phase change caused by expansion, compression and mixing. However, their model's primary and secondary flow was same working fluid with single chemical composition. Cizungu et al. [11] derived two-phase thermodynamic model to calculate the pumping of an ejector. This model can be used both for single-phase and two-phase flow. Zhu and Li [11] derived analytical model for an ejector in a fuel cell recirculation system. Their model used two dimensional velocity profile to better represent a flow inside the mixing tube. However, their model did not consider the condensation effect, instead they simply assumed it as a loss in a total fuel cell system.

In this chapter, main scope is to investigate and analyze the influence

of relative humidity on ejector performance which is a matter of flow condition. A humid air is mixture of vapor and air and when it condenses inside an ejector, it become a two-phase mixture of water, vapor and air. Thus, analyzing an ejector operating with humid air needs different approach compared to methods mentioned above. Main concerns are condensation of vapor and thermos-physical properties of humid gas.

### 2.1.1 Condensation effect

Condensation is the change of the phase from gas to liquid. When humid air meets cool air which has lower temperature than a dew point condensation occurs. Fig. 2.2 shows dew point of secondary flow vs. temperature of primary flow. As relative humidity increases, the dew point of secondary flow is increased. Larger difference between dew point of secondary flow and primary flow, more condensation occurs. The amount of condensed vapor can be calculated by Newton's law of cooling.

$$\dot{m}_c = \frac{q}{h'_{fg}} = \frac{\bar{h}_L A (T_{sat} - T_s)}{h'_{fg}} \quad (2.1)$$

As Eq. (2.1) shows, mass flow rate of condensed vapor increases as temperature difference between dew point and temperature of secondary flow increases.

When condensation occurs, a heat is released. The released heat increases temperature inside the mixing tube of ejector. Thus, as more condensation occurs, exerted heat by condensation increases, decreasing density.

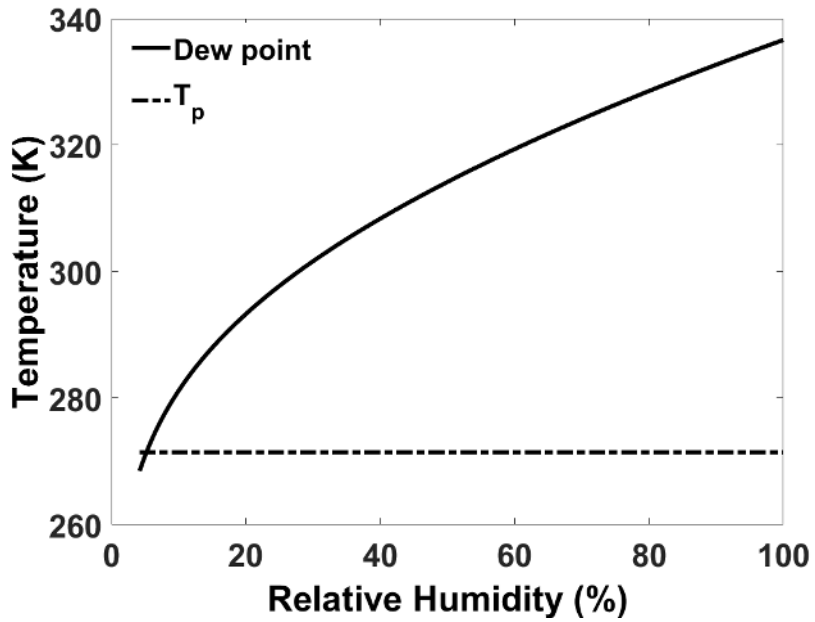


Fig. 2.2. Dew point of secondary flow (330K) vs. primary flow temperature. (300K)

### **2.1.2 Change of thermophysical properties**

The variation of thermophysical properties of air due to humidity is another important factor to consider. Important factors to be considered are density, specific heat capacities and specific heat ratio. Above properties are critical in isentropic relationships which determine flow characteristics in an ejector. Since the properties of humid air strongly depend on temperature and humidity, correlations are needed. For our study, Tsilingiris' correlation [19] which correlates the thermophysical and transportation properties of humid air for a temperature range of 0°C to 100°C and relative humidity range of 0% to 100% have been used. Fig. 2.3, Fig. 2.4, and Fig. 2.5 show the humid air properties of our interest.

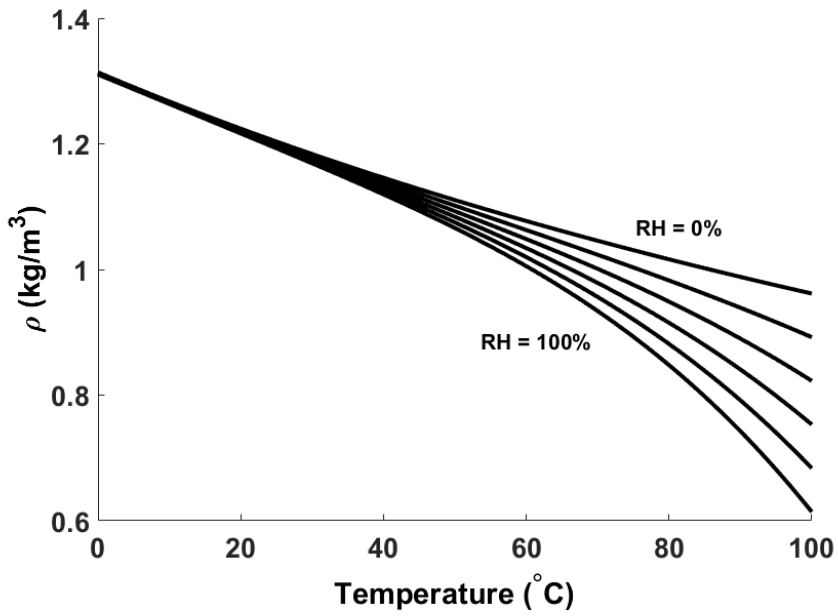


Fig. 2.3. Humidity and temperature effect on density.

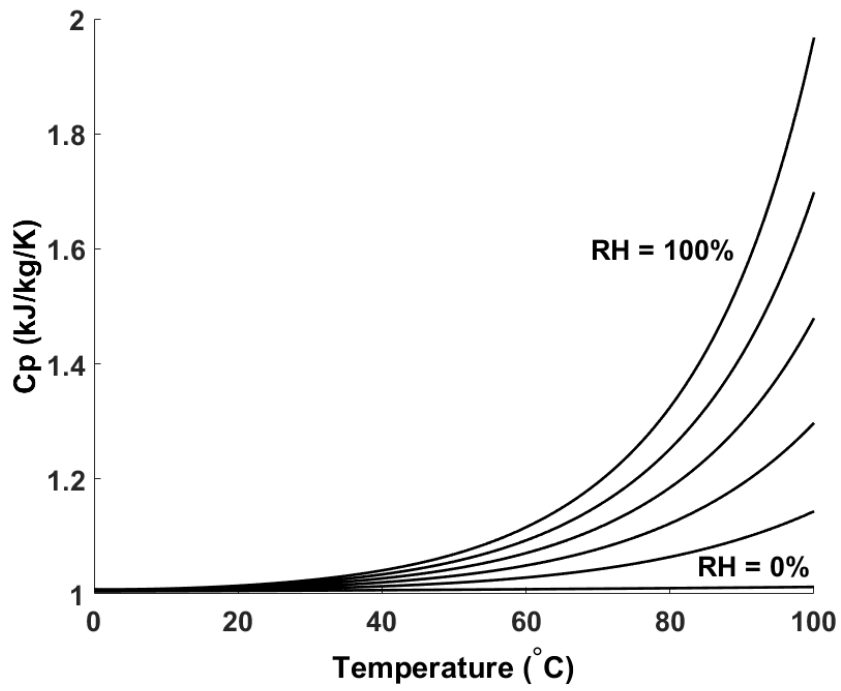


Fig. 2.4. Humidity and temperature effect on specific heat capacity.



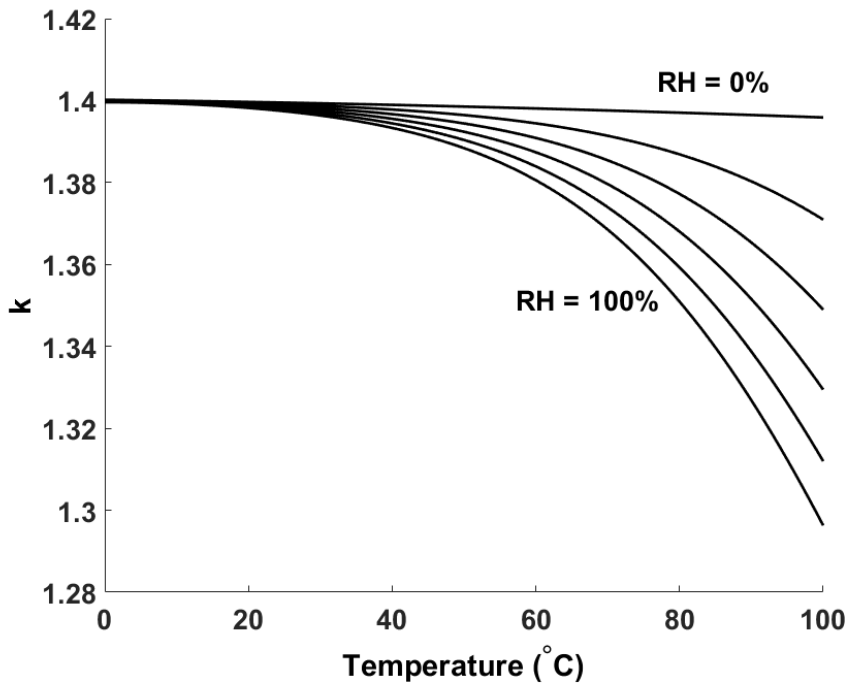


Fig. 2.5. Humidity and temperature effect on specific heat ratio.

Fig. 2.3, 2.4 and 2.5 show the trends of density, specific heat capacity and specific heat ratio. Density decreases as relative humidity rises. Decrease of density would lower the pumping as relative humidity rises. Specific heat capacity tends to increase as relative humidity and temperature increases. Specific heat ratio decreases as relative humidity and temperature increases. This tendency is important because in the ejector design process those properties are extensively used. In n-compound theory. Below is the n-compound flow equation for compressible flow [16].

$$\frac{\dot{m}_j \sqrt{T_{t,j}}}{A_j P_{t,j}} = \left( \frac{P_s}{P_{t,j}} \right) \left\{ \frac{2k}{R(k-1)} \left[ 1 - \left( \frac{P_s}{P_{t,j}} \right)^{\frac{k-1}{k}} \right] \right\} = f \left( \frac{P_s}{P_{t,j}} \right) \quad (2.2)$$

$$\sum_j \left( \frac{A_{j,i}}{A_e} \right) \frac{f_{j,i}}{f_{j,e}} = 1 \quad (2.3)$$

By only accounting variation of thermo-physical and transportation properties (e.g. specific heat ratio) to Eq. (2.2) and (2.3) gives us degradation of pumping up to 5% while increasing relative humidity from 0% to 100%.

## 2.2 Modeling procedure

To model a ‘humid’ air ejector, following assumptions are made.

- i) One dimensional flow
- ii) Steady
- iii) Compressible
- iv) Adiabatic
- v) Fully mixed inside the mixing tube
- vi) Ideal gas

Assumption vi) is valid because at the design point of the ejector, saturation vapor pressure is low enough to be treated as an ideal gas. A control volume of analysis is shown in Fig. 2.6.

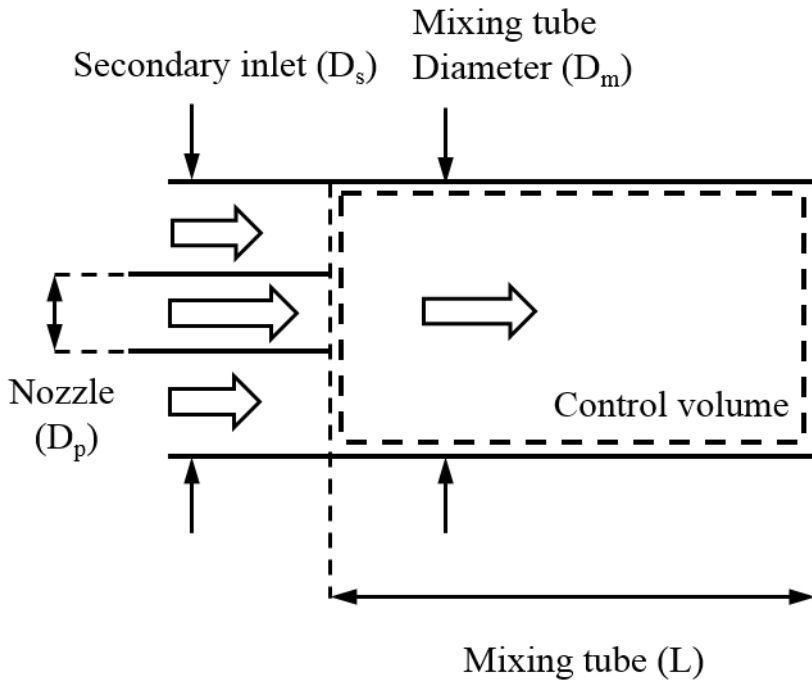


Fig. 2.6. Control volume of analysis.

From given boundary conditions and variables of primary, secondary and exit flow, the model outputs mass flow rate of secondary flow. The main variable is a relative humidity of secondary flow. For each relative humidity of secondary flow, the Mach number of secondary flow is obtained thus pumping of the ejector is calculated. Since humid air properties are function of pressure, temperature and relative humidity, correlations for thermos-physical properties are required for the model. In this study, Tsilingiris' correlations [19] were used. To start iteration

procedure, the Mach number of secondary flow is assumed. In this study, Mach number of 0.1 was selected to match designed value. The velocity of primary flow is calculated with a given mass flow rate, area and density.

$$\dot{m}_p = \rho_p u_p A_p \quad (2.4)$$

$$u_p = \frac{\dot{m}_p}{\rho_p A_p} \quad (2.5)$$

Mach number of the primary flow is

$$Ma_p = \frac{u_p}{a_p} \quad (2.6)$$

Static temperature and pressure of the primary flow can be obtained from isentropic relations.

$$T_{s,p} = \frac{T_{t,p}}{1 + 1/2(k_p - 1)Ma_p^2} \quad (2.7)$$

$$P_{s,p} = \frac{P_{t,p}}{\left(1 + 1/2(k_p - 1)Ma_p^2\right)^{k_p/(k_p - 1)}} \quad (2.8)$$

The static pressures of both the primary and secondary flows are the same at the mixing tube entrance.

$$P_{s,p} = P_{s,s} \quad (2.9)$$

Static temperature of the secondary flow can be obtained using equation of state.

$$P_{s,p} = \rho_s (k_s - 1) c_{v,s} T_{s,s} \quad (2.10)$$

$$T_{s,s} = \frac{P_{s,s}}{\rho_s (k_s - 1) c_{v,s}} \quad (2.11)$$

Using isentropic relations, the Mach number of the secondary flow is given as:

$$Ma_s = \sqrt{\left(\frac{2}{k_s - 1}\right) \left[ \left(\frac{P_{t,s}}{P_s}\right)^{(k_s - 1)/k_s} - 1 \right]} \quad (2.12)$$

Then Greitzer's substitution principle for two-stream mixing model is used [20] to calculate velocity of secondary flow. To use the similarity principle, the following non-dimensional factors are needed.

$$\theta = \frac{T_{s,s}}{T_{s,p}} \quad (2.13)$$

$$\chi = \frac{P_{t,s} - P_{t,p}}{\frac{1}{2}(\rho_s u_s^2)_i} \quad (2.14)$$

Then the velocity ratio is obtained from substitution principle as:

$$\frac{u_{s,i}}{u_{p,i}} = \sqrt{\theta(1-\chi)} \quad (2.15)$$

$$u_{s,i} = u_{p,i} \sqrt{\theta(1-\chi)} \quad (2.16)$$

Thus, the Mach number of the secondary flow is:

$$Ma_{s,i} = \frac{u_{s,i}}{a_s} \quad (2.17)$$

The mass flow rate of the vapor in ejector is calculated from the definition of relative humidity and absolute humidity.

$$RH_s = \frac{P_v}{P_{sv}} \quad (2.18)$$

$$AH_s = \frac{\dot{m}_v}{\dot{m}_s} = \frac{M_v}{M_a} \frac{P_v}{P_s} = \frac{(M_v/M_a) RH_s}{P_s/P_{sv} - RH_s} \quad (2.19)$$

$$\dot{m}_v = \dot{m}_s \left( \frac{M_v}{M_a} \right) \left( \frac{P_{sv}}{P_s} \right) \quad (2.20)$$

From the mass flow rate of vapor, the absolute humidity at the exit is:

$$AH_e = \frac{\dot{m}_v}{\dot{m}_s + \dot{m}_p} \quad (2.21)$$

With the absolute humidity known, the relative humidity at exit is calculated as:

$$RH_e = \frac{(P_s/P_{sv})AH_e}{M_v/M_a + AH_e} \quad (2.22)$$

From the known relative humidity at exit, air properties at exit can be calculated. Condensation occurs when humid air meets cold flow at a temperature lower than the dew point of the humid air. In this case the primary flow's temperature is lower than the secondary flow's dew point temperature. The condensed water's mass flow rate is obtained using the latent heat of water and the enthalpy difference between the inlet and exit.

$$\dot{m}_c h_{fg} = h_p + h_s - h_e \quad (2.23)$$

The heat release from condensation also increases the secondary flow's temperature in the mixing tube. The latent heat of the vapor can be expressed with the Jakob number, which relates the temperature of the primary flow and the dew point temperature of the secondary flow.

$$Ja = \frac{c_{p,liquid} (T_p - T_{sat})}{h_{fg}} \quad (2.24)$$

Jakob number's physical meaning is the ratio of sensibility to the latent energy absorbed during the liquid-vapor phase change. From



Nusselt [21] and Rohsenow's [22] studies, an accurate value of the latent heat is a function of the Jakob number.

$$h'_{fg} = h_{fg} (1 + 0.68Ja) \quad (2.25)$$

Thus, the temperature rise of the secondary flow can be written as:

$$\Delta T = \frac{\dot{m}_c h'_{fg}}{\dot{m}_s c_{p,s}} \quad (2.26)$$

A pressure drop occurs as vapor in the mixing tube condensate. The partial pressure of vapor decreases pressure inside the mixing tube. using Raoult's law, pressure drop due to condensation is obtained by following equation.

$$\Delta P_v = \frac{\dot{m}_c}{\dot{m}_s} \frac{M_a}{M_v} P_{s,s} \quad (2.27)$$

With temperature rise and pressure drop due to condensation are then used to update the initially calculated temperature and pressure for the secondary for further iteration until conservation laws are satisfied.

## 2.3 Conclusions

A new model of ‘humid’ ejector has been developed. It is based on isentropic relations, correlation of humid air’s thermo-physical properties and heat release by condensation. The model’s calculation procedure is as follows.

First, boundary conditions and initial flow properties are needed. Based on assumed Mach number of secondary flow, flow properties such as density and specific heat ratio are calculated using correlation. With given conditions above, velocity, temperature and pressure of both primary and secondary flow are calculated. Using two stream mixing model and mass conservation of vapor, flow properties and characteristics at the exit of an ejector are obtained. With calculated inlet condition and exit condition, the mass, momentum and energy conservation are checked. If the calculated result does not match conservation laws, Mach number and temperature of secondary flow are updated and iterate until conservation laws are satisfied. Fig. 2.7 shows the summarized calculation procedure.

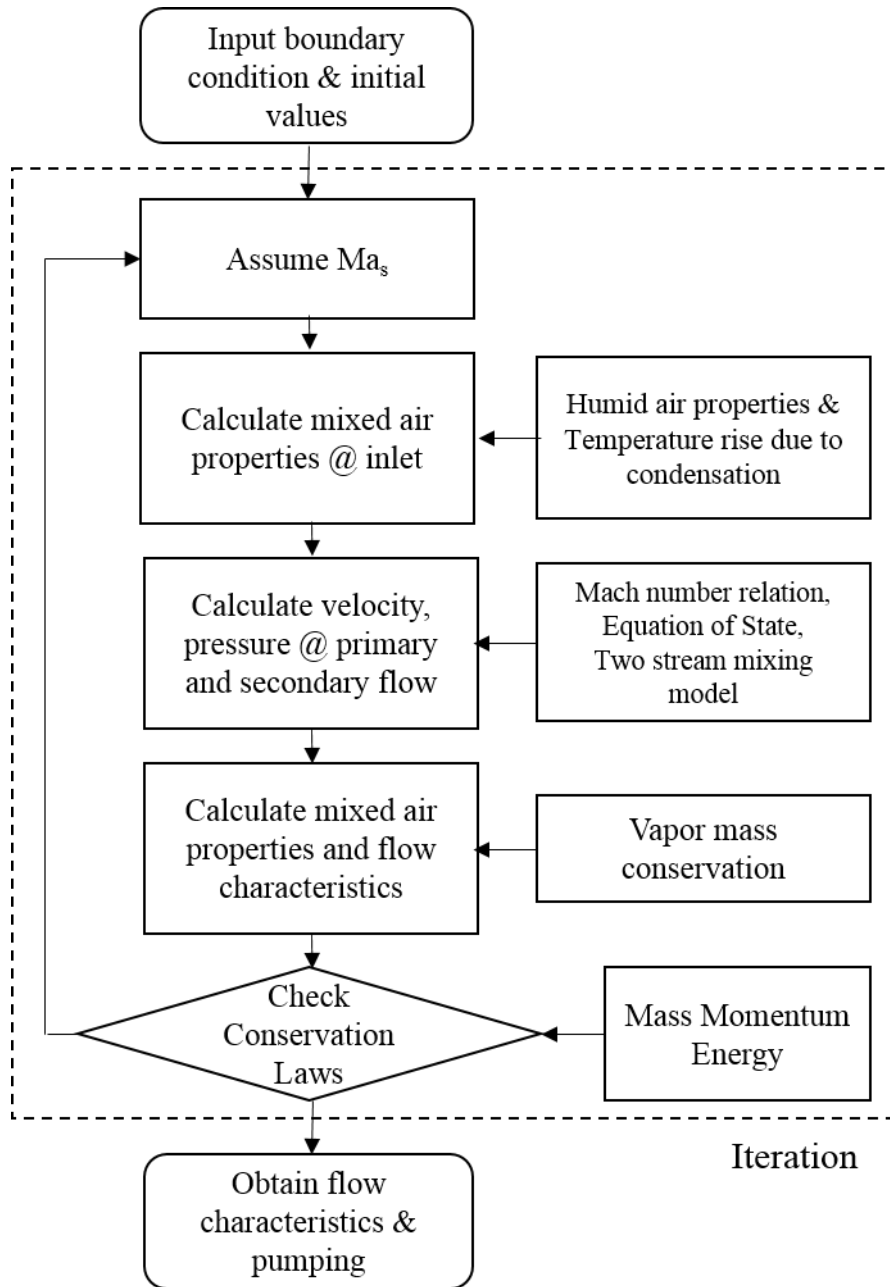


Fig. 2.7. Analysis flow chart.

## **Chapter 3.**

# **Measurement of Pumping Degradation**

## **due to Humidity**

### **3.1 Introduction**

In this chapter, pumping degradation of ejector due to humidity has been measured. The ejector discussed in this chapter is designed as part of fuel recirculator in a fuel cell automobile. In a fuel cell, its efficiency is directly related to stack voltage. Stack voltage suffers various losses and one of the loss is concentric loss. To overcome concentric loss, excessive hydrogen and air is supplied to the fuel cell stack. This excessive hydrogen supply however, creates unreacted hydrogen and vapor. In order to increase efficiency of fuel cell, an ejector that recirculates excess hydrogen is required. However, due to vapor in recirculated flow, an ejector faces humid secondary flow. Studies on fuel recirculating ejector has been done by several researchers. Marsano et al. [12] designed and analyzed an ejector performance and off-design behavior. The ejector they analyzed is part of recirculation system used

in SOFC system. However, their model assumed perfect dry hydrogen supply. Kim et al. [13] designed and tested fuel recirculation ejector as part of submarine PEMFC system. They developed an analytical model which design optimal geometry and flow condition. Their design procedure assumed homogeneous mixture of hydrogen and water vapor as a working fluid. To validate their model, they used mock-up setting experiment to validate their model. They used hydrogen as a working fluid and installed pressure regulator at the exit to represent pressure drop at the fuel cell stack inlet. Zhu and Li [14] developed 2-D model for an ejector used in PEM fuel cell system including humidifier installed at exit of ejector. They used two dimensional velocity profile to improve prediction of an ejector performance. The velocity distribution was obtained by CFD method. However, their model did not consider humidity change in the system. Engelbracht et al. [15] modeled and compared a fuel driven ejector and steam driven ejector used in SOFC fuel recirculation system. They modeled working fluid as a function of a fuel utilization ratio. However, the working fluid was described in terms of fuel utilization ratio rather than relative humidity. However, the effect of humid secondary flow on ejector performance has not been studied. This chapter presents experiment result of a ‘humid’ ejector and validate the new analytical model.

## **3.2 Experiment of an ejector with humid secondary flow**

An ejector for fuel cell automobile was designed and tested in this study. Since experiment using hydrogen is dangerous, an ejector using air as a working fluid with same Reynolds number and Mach number has been designed and tested. The design process of an ejector is described in part 3.2.2.

### **3.2.1 Experiment setup**

An experiment setup has been built to test the designed ejector. The schematic of experiment setup is shown in Fig. 3.1. Photo of the ejector test setup is shown in Fig. 3.2. Fig. 3.3 shows the manufactured test ejector. The ejector was manufactured by CNC machining and its material is stainless steel. The experiment setup consists of ejector, compressed air tanks, pressure chamber, humidifier and sensors. Photos of compressed air tanks and pressure chamber are shown in Fig. 3.4 and Fig. 3.5. Sensors used in the experiment are listed in table 3.1. Photos of sensors used in experiment are shown in Fig. 3.6 to Fig. 3.9. A pressure chamber provides air to both the primary and secondary flows of the ejector. Dry air (4% of relative humidity (RH)) has been supplied for the primary flow. In the inlet of the primary flow, pressure transducer,

thermocouple, and volume flow rate meter has been installed. At the inlet of the secondary flow, pressure transducer and volume flow rate meter has been installed. To control the mass flow rate, needle valves installed at the inlet of primary has been used. The secondary flow is humidified by a custom built humidifier.

Table 3.1. List of sensors used in experiment setup.

Model name	Specification	Usage
GR112-1-A-PO	Range: 0-20 SLPM Accuracy: 1% F.S.	Mass flow rate (Primary flow)
822-13-OV1-PVI-V1	Range: 0-15 SLPM Accuracy: 1.5% F.S.	Mass flow rate (Secondary flow)
FPA	Range: 0-100psi (abs) Accuracy: 0.1% F.S.	Pressure (Primary and exit)
BARATRON 698A13TRA	Range: 0-1000Torr Accuracy: 0.05% F.S.	Pressure (Secondary flow)
Thermocouple (K-type)	Accuracy: $\pm 1.0K$	Temperature



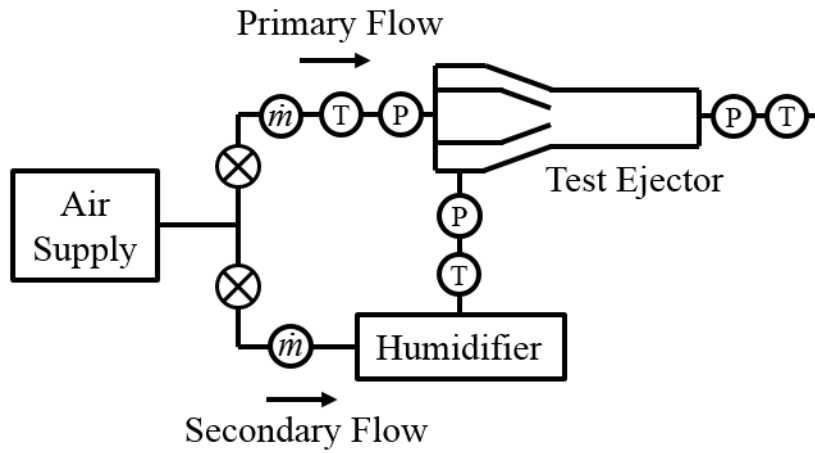


Fig. 3.1. Schematic of the experiment setup.

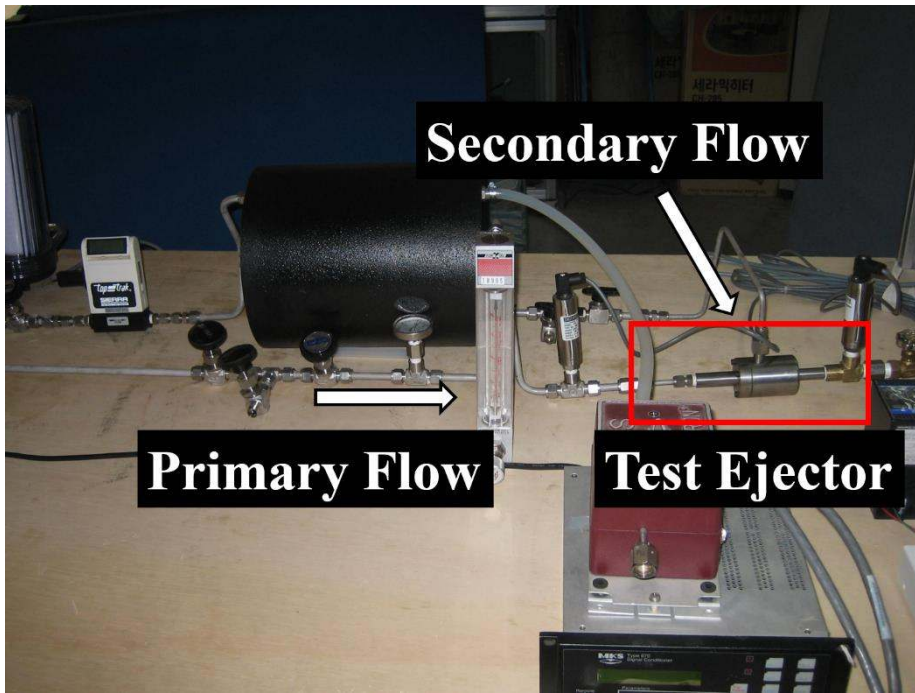


Fig. 3.2. Photo of the experiment setup.



Fig. 3.3. Photo of the test ejector.



Fig. 3.4. Compressed air tanks.



Fig. 3.5. Pressure chamber.



Fig. 3.6. Mass flow rate meter used in primary flow  
(GR112-1-A-PO).



Fig. 3.7. Mass flow rate meter used in secondary flow  
(GR112-1-A-PO).



Fig. 3.8. Pressure sensor used in primary and exit flow (FPA).





Fig. 3.9. Pressure sensor used in secondary flow  
(BARATRON 698A13TRA).

A humidifier was built to provide humid air to secondary flow. The humidifier is an electrode type humidifier which generates vapor by supplying an AC current through the electrode. A resistance type humistor has been installed to measure and control relative humidity. A resistance type humistor varies its electric resistance as relative humidity changes. To control humidity and temperature, a heat exchanger has been installed. The flow of water inside the heat exchanger has been controlled to vary the relative humidity and temperature. To obtain humid air, water vapor and air have been mixed. In the dehumidifying process, a cooler with cooled water has been used to decrease the temperature of the inlet air below the dew point. For the tubing between the humidity controller and the ejector, a heater was installed to maintain a constant temperature. Detailed specification of the humidifier is shown in Table 3.2. Schematic of humidifier is shown in Fig. 3.10. A photo of the humidifier is shown in Fig. 3.11. Part description of humidifier is presented in Table 3.3.

Table 3.2. Specification of the humidifier.

Operating temperature	0-55°C
Operating relative humidity	0-100%
Operating mass flow rate	3-30LPM
Accuracy (temperature)	±1°C
Accuracy (relative humidity)	±1%
Control method	Linear control

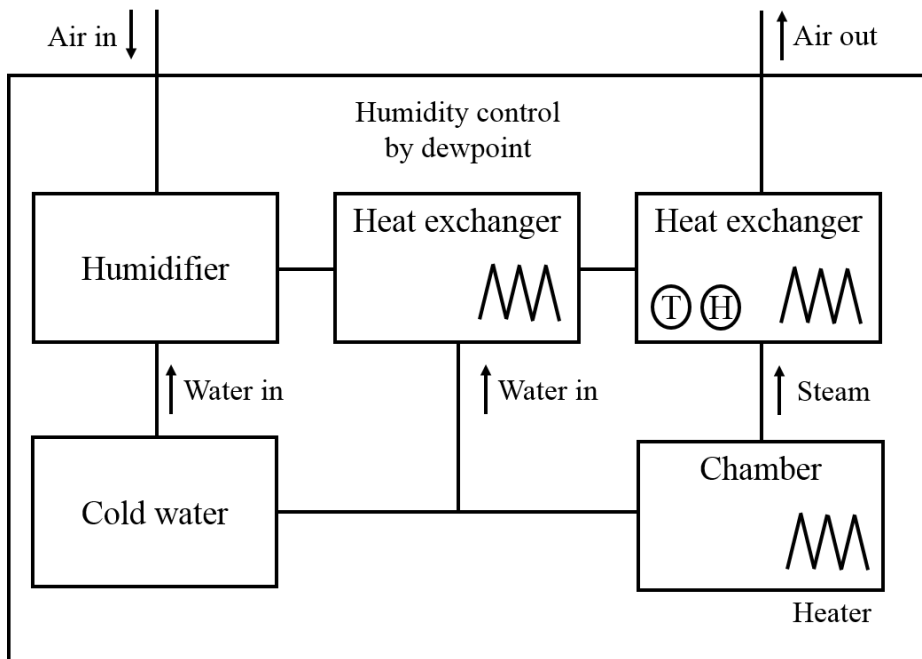


Fig. 3.10. Schematic of the humidifier.

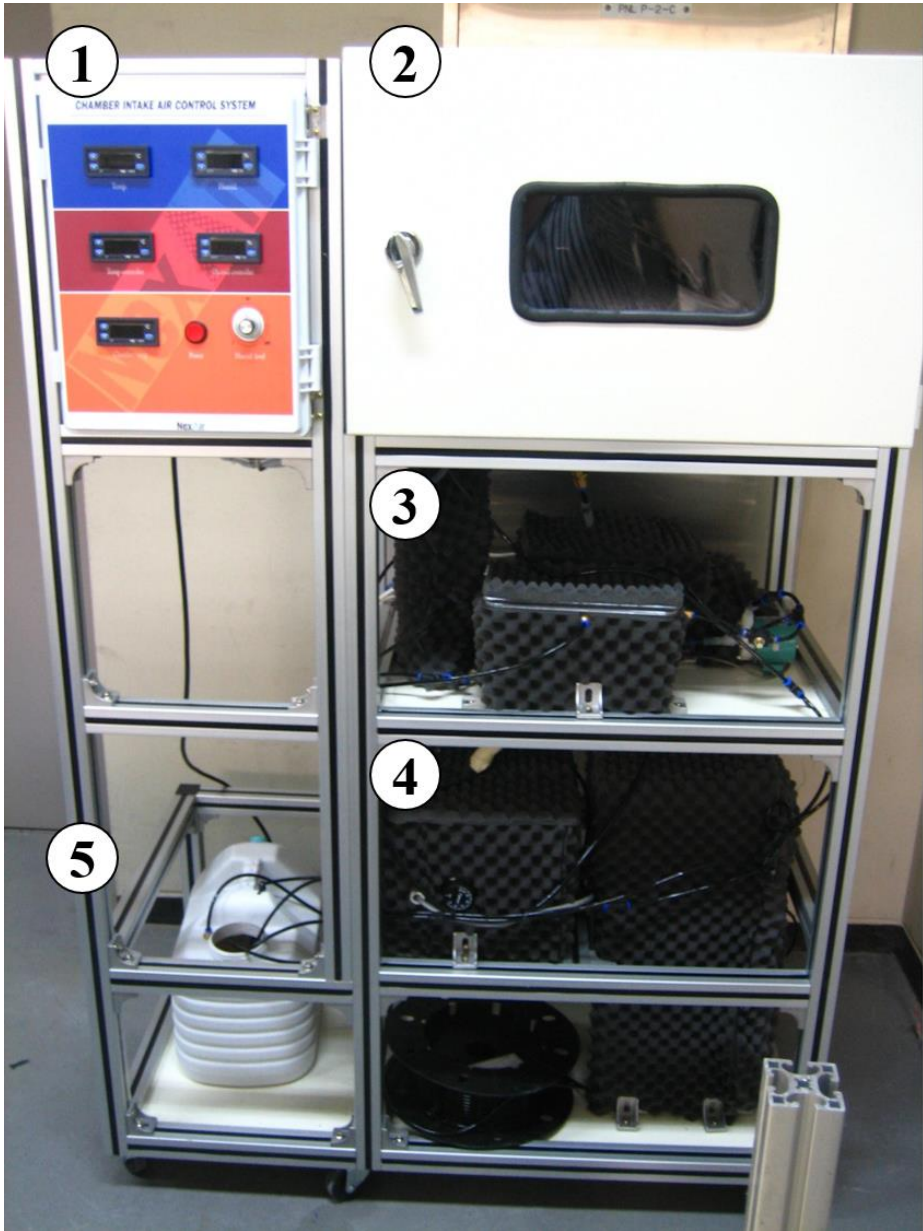

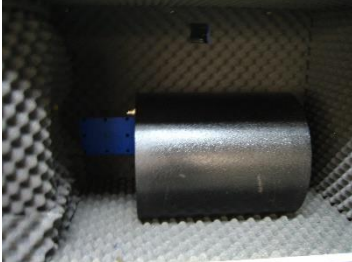


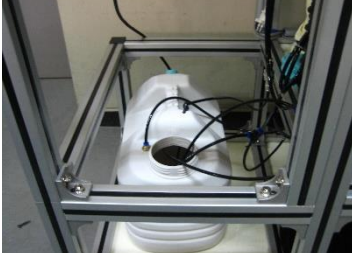


Fig. 3.11. Photo of the humidifier.

Table 3.3. Part descriptions of the humidifier.

Number	Photo	Description
1		Control Panel
2		Chamber
3		Heat exchanger (dewpoint control)
4		Heat exchanger and humidifier
5		Water tank

### 3.2.2 Ejector design

An ejector is a simple pump which has no moving parts. It contains primary nozzle, secondary flow inlet, mixing tube and diffuser. The primary flow entrains secondary flow by its energy and two flows are mixed in mixing chamber.

An ejector can be classified in two different ways. First classification is related to primary nozzle flow's velocity; supersonic versus subsonic. As shown in Fig. 3.12, subsonic ejector has convergent nozzle while supersonic ejector has convergent-divergent nozzle. Supersonic ejector has larger entrainment compared to subsonic ejector but supersonic ejector's nozzle is more difficult to manufacture. Second classification is about mixing tube geometry; constant pressure mixing tube versus constant area mixing tube. Fig. 3.13 shows schematic of two different types of an ejector based on shape of a mixing tube. Constant pressure mixing tube is better in terms of ejector efficiency but it is difficult to design and manufacture. Also, an ejector used in fuel cell automobile requires subsonic flow at the fuel stack inlet. [14] In this study, an ejector with subsonic flow, constant area mixing tube was designed and tested.

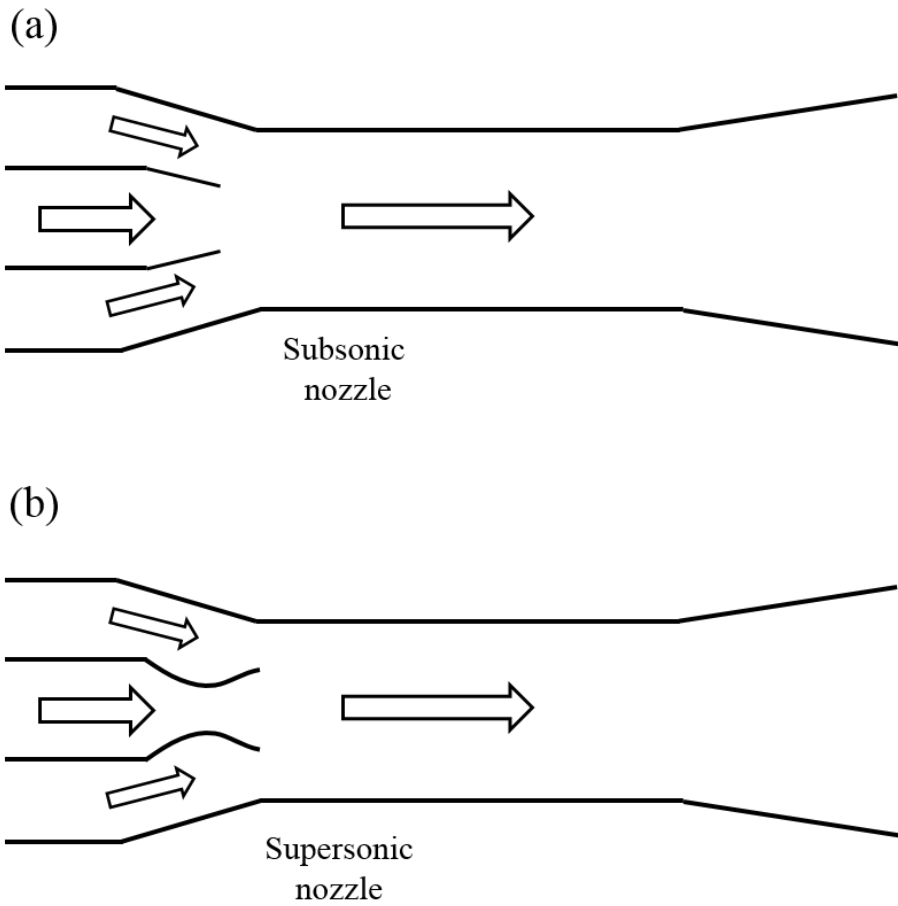


Fig. 3.12. Two types of an ejector nozzle.

(a) subsonic nozzle, (b) supersonic nozzle.



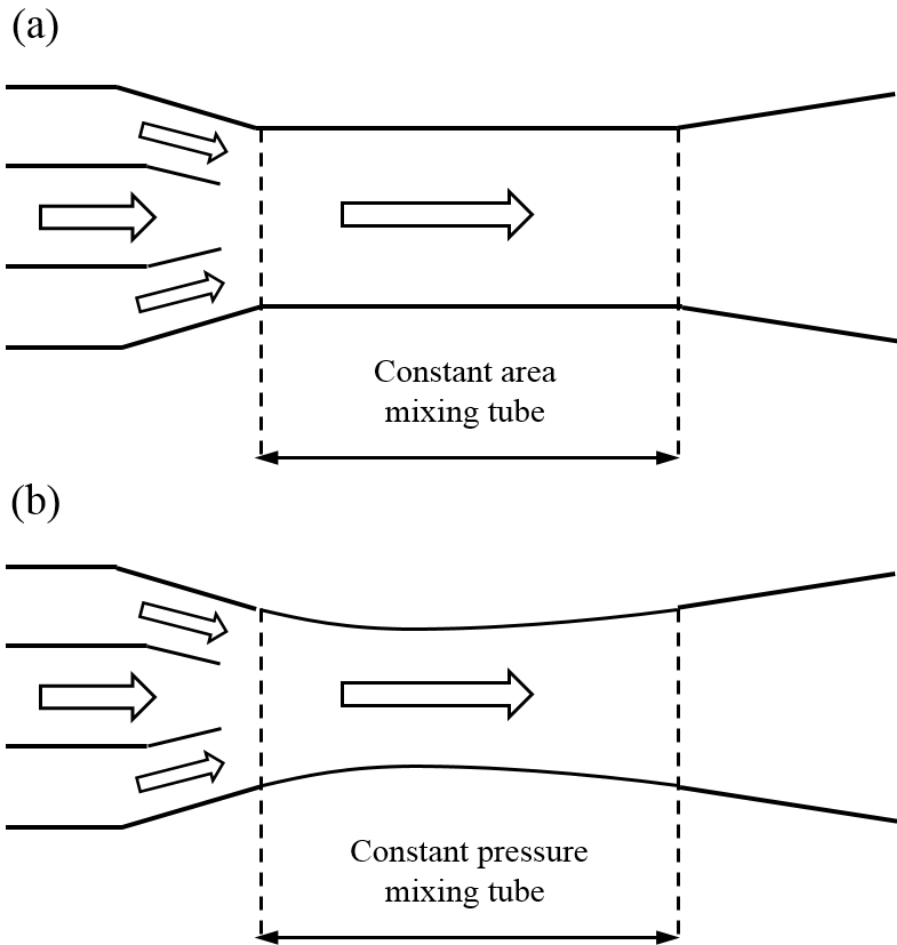


Fig. 3.13. Two types of an ejector mixing tube.

(a) constant area mixing, (b) constant pressure mixing

In this study, the ejector was designed for 80kW class automobile. In order to calculate mass flow rate of fuel, following equation is used.

$$\dot{m}_{H_2} = \frac{IN}{2F} \cdot \lambda \cdot M_{H_2} \quad (3.1)$$

I is the electric current of the fuel cell and N is number of fuel cell stack. F is the Faraday constant. The Stoichiometric constant  $\lambda$  gives secondary mass flow rate. It is a ratio of additionally supplied hydrogen which is often used to increase efficiency of the fuel cell.

$$\lambda = \frac{\dot{m}_{H_2,feed}}{\dot{m}_{H_2,consumed}} > 1 \quad (3.2)$$

In this study,  $\lambda$  of 1.2 was chosen. In order to determine ejector's pressure, temperature and geometry, following assumptions were made; steady, ideal gas with constant specific heats and isentropic. From requirements of fuel cell stack, primary flow's temperature, secondary flow's pressure and temperature, and exit flow's temperature are given. To design subsonic-constant area mixing ejector, following isentropic relations are needed.

$$\frac{P_{t,p}}{P_{s,p}} = \left(1 + \frac{k-1}{2} Ma_p^2\right)^{\frac{k}{k-1}} \quad (3.3)$$

By setting total pressure of primary value, Mach number of primary flow

is obtained.

$$Ma_p = \sqrt{\frac{2}{k-1} \left( \left( \frac{P_{t,p}}{P_{s,p}} \right)^{\frac{k-1}{k}} - 1 \right)} \quad (3.4)$$

As Mach number of primary flow is obtained, temperature, density and velocity of primary flow can be calculated by following equations.

$$\frac{T_{t,p}}{T_{s,p}} = 1 + \frac{k-1}{2} Ma_p^2 \quad (3.5)$$

$$\frac{\rho_{t,p}}{\rho_{s,p}} = \left( 1 + \frac{k-1}{2} Ma_p^2 \right)^{\frac{1}{k-1}} \quad (3.6)$$

$$u_p = Ma_p \sqrt{kRT_{s,p}} \quad (3.7)$$

From given mass flow rate of primary flow nozzle area is determined.

$$A_p = \frac{\dot{m}_p}{\rho_p u_p} \quad (3.8)$$

To obtain secondary flow characteristics, n-compound flow theory by Greitzer et al. [16] and below equations are used.

$$\frac{\dot{m}_j \sqrt{T_{t,j}}}{A_j P_{t,j}} = \left( \frac{P_s}{P_{t,j}} \right)^{\frac{1}{k}} \left\{ \frac{2k}{R(k-1)} \left[ 1 - \left( \frac{P_s}{P_{t,j}} \right)^{\frac{k-1}{k}} \right] \right\}^{\frac{1}{2}} = f \left( \frac{P_s}{P_{t,j}} \right) \quad (3.9)$$

Summing the stream areas at the exit:

$$\frac{\dot{m}_p \sqrt{T_{t,p}}}{P_{t,p} f_{p,e}} + \frac{\dot{m}_s \sqrt{T_{t,s}}}{P_{t,s} f_{s,e}} = A_e \quad (3.10)$$

By using Eq. (3.7) and Eq. (3.8), flow characteristics of secondary flow and exit flow can be obtained. Since experiment using hydrogen is dangerous, an ejector using air as a working fluid was designed by matching Mach number. Table 3.3 shows designed ejector's major characteristics. Fig. 3.14 shows three dimensional view of the designed ejector. Fig. 3.15 to Fig. 3.19 shows drawings of the designed ejector.

Table 3.3. Designed ejector.

Station	Design Parameter	Value
Primary Flow	Mass Flow Rate ( $\dot{m}_p$ )	1.74 g/s
	Total Pressure ( $P_{t,p}$ )	175 kPa
	Total Temperature ( $T_{t,p}$ )	298.15 K
	Nozzle Diameter ( $D_p$ )	2.4 mm
Secondary Flow (design point)	$\dot{m}_s/\dot{m}_p$	0.18
	$P_{t,s}/P_{t,p}$	0.58
	$T_{t,s}/T_{t,p}$	1.10
	$D_s/D_p$	2.17
Exit Flow	$P_{t,e}/P_{t,p}$	0.58

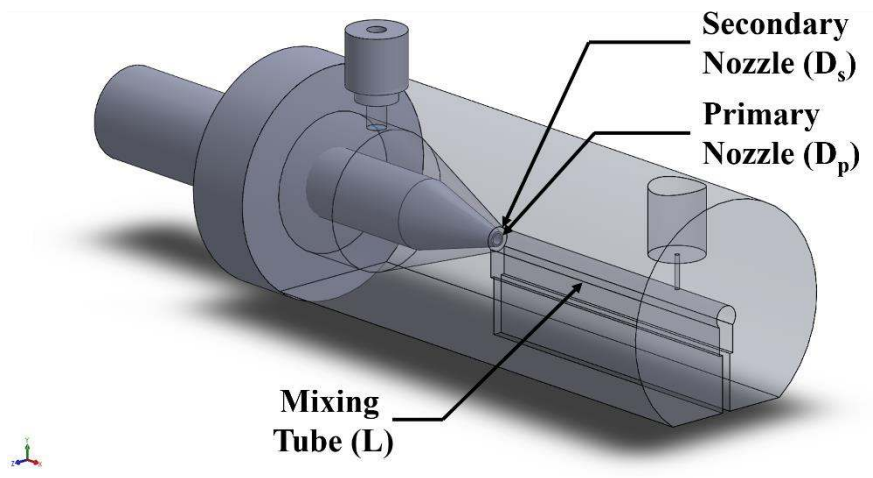


Fig. 3.14. Three-dimensional view of the designed ejector.

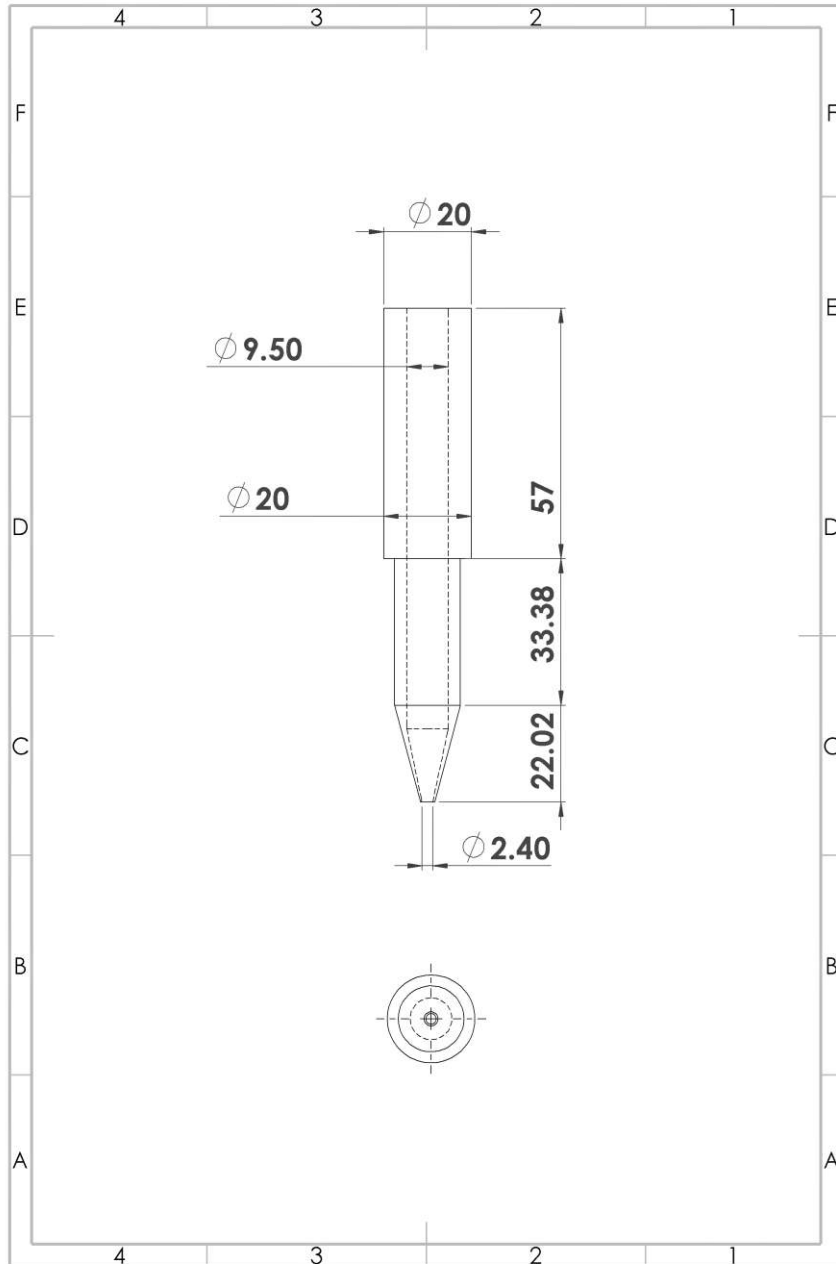


Fig. 3.15. Primary nozzle.

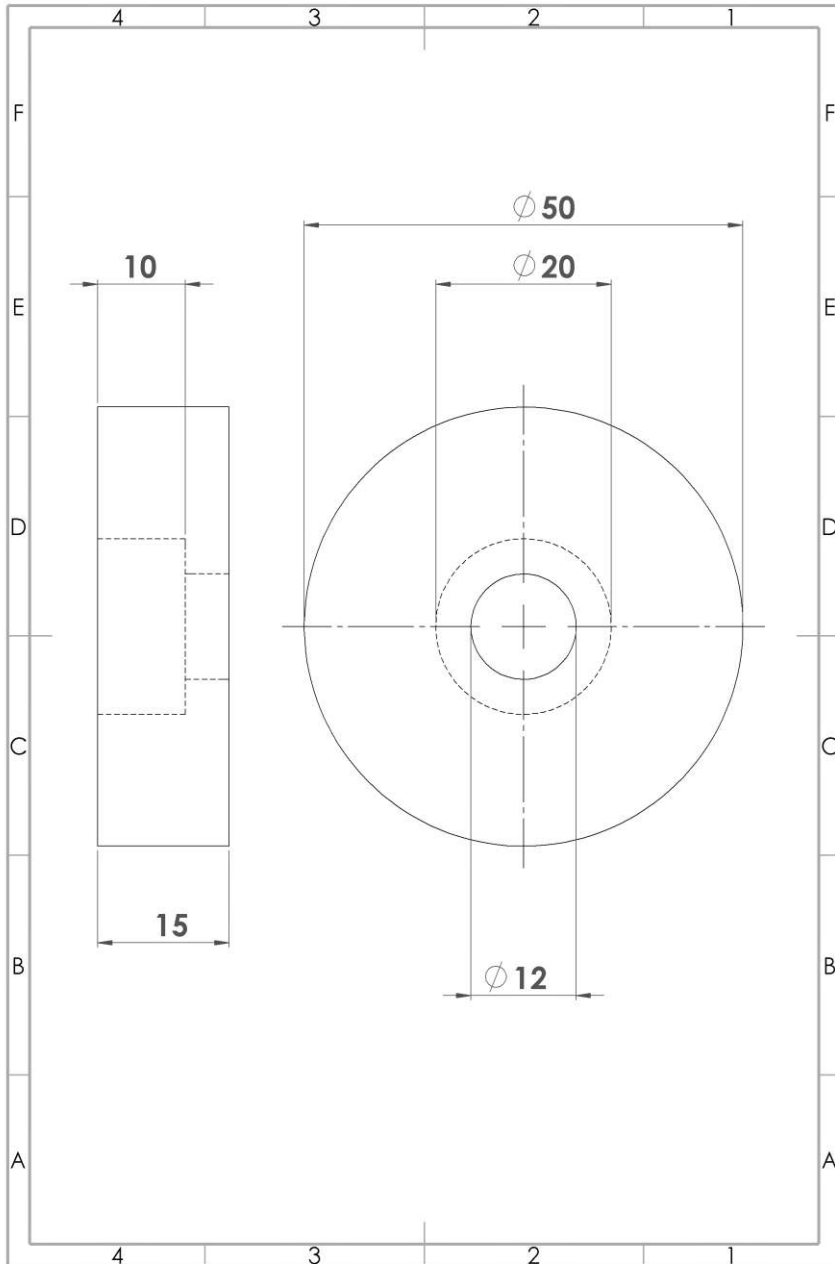


Fig. 3.16. Nozzle holder.



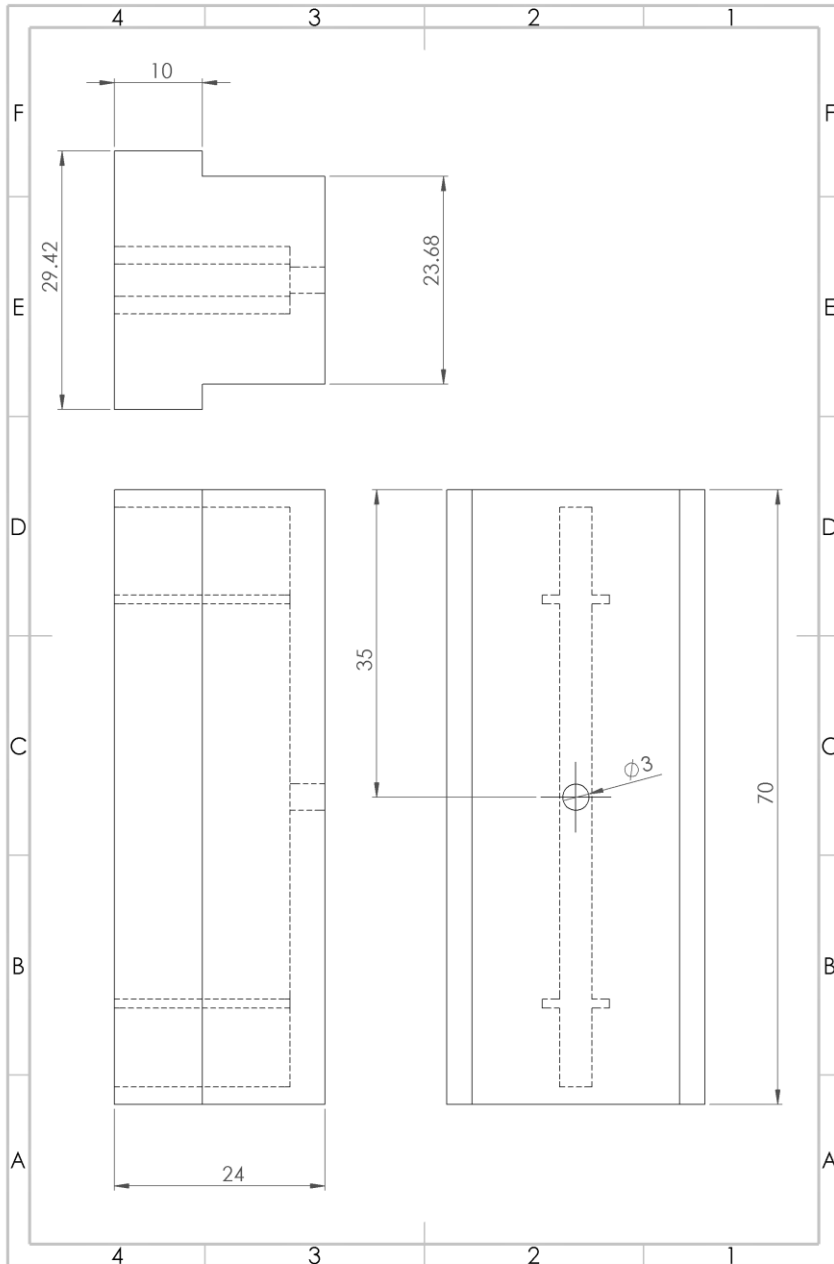


Fig. 3.17. Mixing chamber sealing.

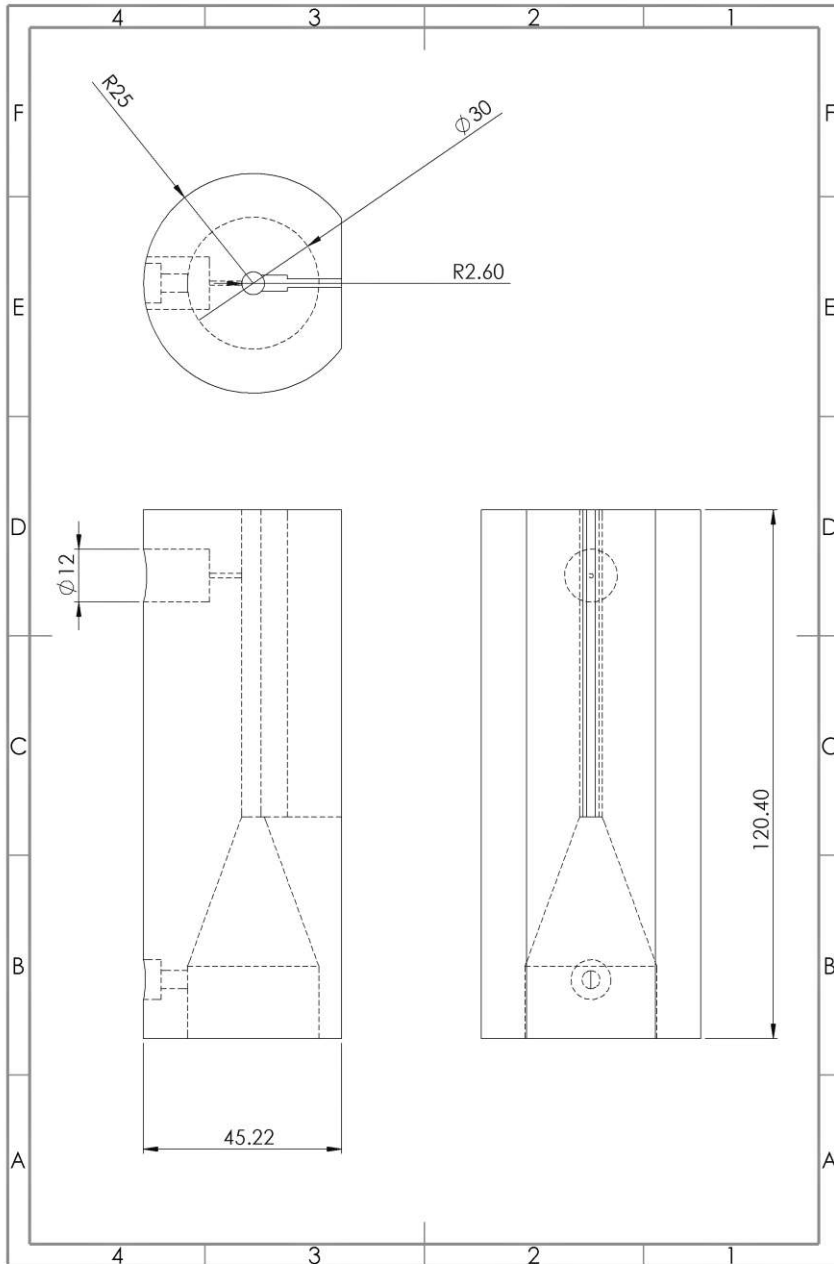


Fig. 3.18. Mixing chamber.

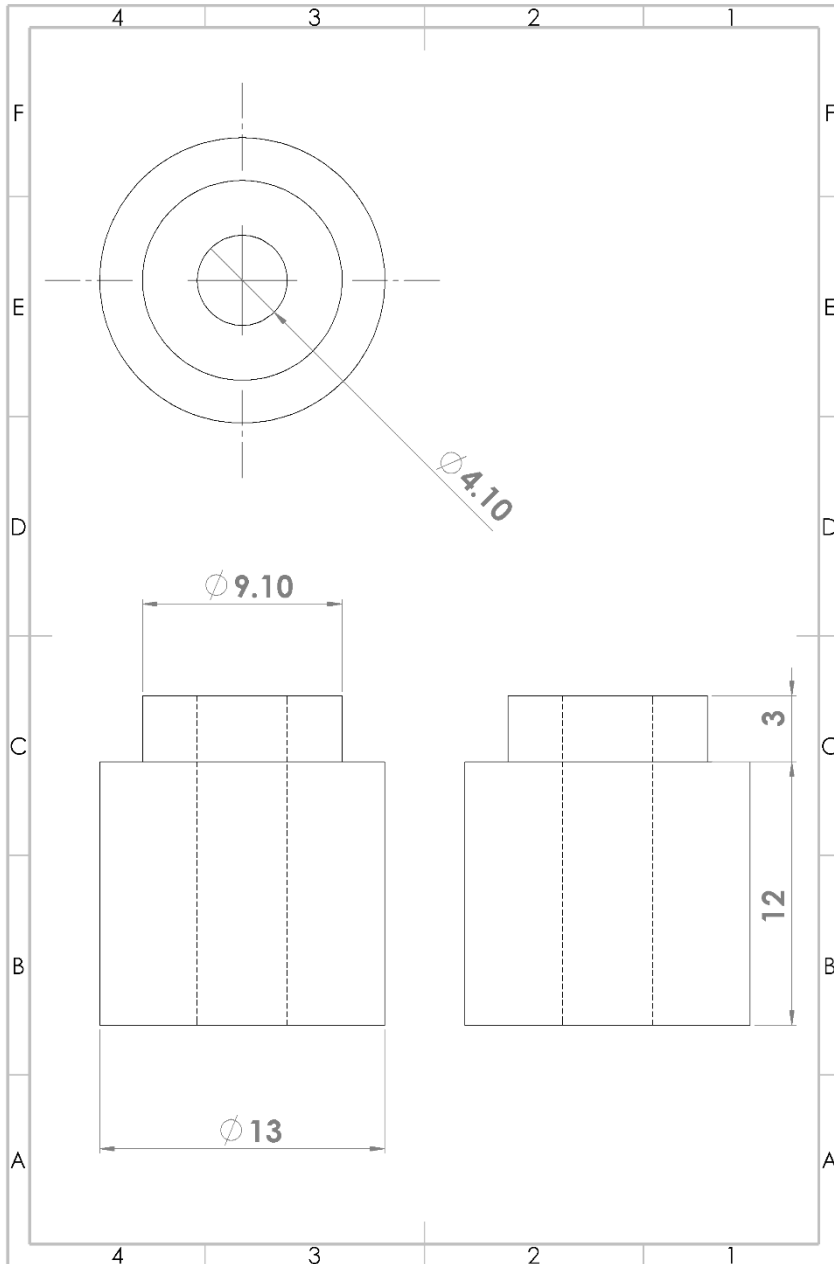


Fig. 3.19. Secondary flow inlet.

### 3.2.3 Uncertainty Analysis

Uncertainty analysis was performed for an experiment. Flow characteristics to be measured are mass flow rate, pressure and temperature. Consider a general case uncertainty given by a test result [17].

$$U_r = \left[ \sum_{i=1}^j \frac{\partial r}{\partial X_i} U_{x_i} \right]^{1/2} \quad (3.11)$$

A mass flow rate can be expanded as below by considering instrumentation listed in Table 3.1.

$$\dot{m} = \rho \dot{V} \quad (3.12)$$

A density is function of pressure and temperature from equation of state.

$$\rho = \frac{P}{RT} \quad (3.13)$$

Summing up Eqs. (3.11) to (3.13), uncertainty of mass flow rate can be expressed as below.

$$\frac{U_{\dot{m}}}{\dot{m}} = \sqrt{\left(\frac{U_P}{P}\right)^2 + \left(\frac{U_T}{T}\right)^2 + \left(\frac{U_{\dot{V}}}{\dot{V}}\right)^2} \quad (3.14)$$

With same manner, uncertainty of relative humidity can be obtained. The uncertainty of derived relative humidity generated by humidifier can be

estimated by accuracy of dew point sensor and relative humidity sensor.

[18] Uncertainties of dew point and relative humidity can be expressed as below.

$$U_{RH} = \sqrt{\left(\frac{\partial RH}{\partial T} U_T\right)^2 + \left(\frac{\partial RH}{\partial T_d} U_{T_d}\right)^2} \quad (3.14)$$

$$U_{T_d} = \sqrt{\left(\frac{\partial T_d}{\partial T} U_T\right)^2 + \left(\frac{\partial T_d}{\partial RH} U_{RH}\right)^2} \quad (3.15)$$

The uncertainty (with confidence level of 95%) of a mass flow rate is 2.14% and the uncertainty of a relative humidity is 2.13% at the design point.

### 3.3 Test result

Before testing an ejector using a humidifier, experiment using dry air was conducted to compare with design value. Total pressure, temperature, and mass flow rate of the primary flow has been fixed to the design point. Pressure and mass flow rate has been controlled using valves installed upstream of the primary flow. Then pressure and temperature of the secondary flow has been fixed. Exit total pressure and temperature also has been fixed to the design point. Then the mass flow rate of entrained secondary flow has been measured. An experiment result using dry air is shown in table 3.4. As shown in table 3.4, experiment result shows good agreement with the design.

Table 3.4. Experiment result at design point for zero relative humidity.

Station	Flow Characteristics	Design Value	Measured Value
Primary Flow	Mass Flow Rate	1.74 g/s	1.734 g/s
	Pressure	175 kPa	178 kPa
	Temperature	298.15 K	298 K
Secondary Flow	$\dot{m}_s/\dot{m}_p$	0.18	0.19
	$P_{t,s}/P_{t,p}$	0.58	0.58
	$T_{t,s}/T_{t,p}$	1.10	1.10
Exit Flow	$P_{t,e}/P_{t,p}$	0.58	0.58
	$T_{t,e}/T_{t,p}$	1.00	1.01

The second experiment with humid secondary flow was conducted. The primary flow conditions have been fixed to design point. In addition, stagnation pressure and temperature of have been also fixed to the design point. Then by varying secondary flow's relative humidity from 4% to 77%, mass flow rate of secondary flow was measured. Fig. 3.20 and Table 3.5 shows test result. The pumping decreases as relative humidity increases where pumping of secondary flow is define as follows:

$$\Phi = \frac{\dot{m}_s}{\dot{m}_{s,design}} \quad (3.16)$$

In the experiment, condensed water has been observed at the exit of the ejector. It suggests that during a mixing process, condensation occurs as the new model predicts. Photo of condensed water at the ejector exit is shown in Fig. 3.21.



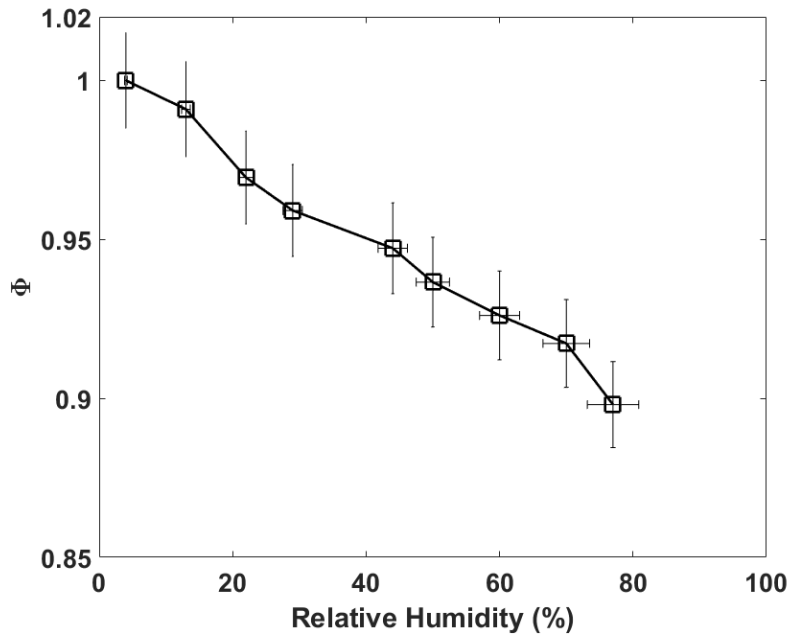


Fig. 3.20. Measured pumping of secondary flow vs. relative humidity.

Table 3.5. Experiment data using humid secondary flow.

Relative humidity (%)	Mass flow rate (g/s)	Pumping
4	0.385	1.000
13	0.381	0.991
22	0.373	0.970
29	0.369	0.959
44	0.364	0.947
50	0.360	0.937
60	0.356	0.926
70	0.353	0.917
77	0.345	0.900



Fig. 3.21. Condensed water at the ejector exit.

### 3.4 Conclusions

The conclusions of this chapter can be summarized as follows.

1. A test facility to measure the effects of relative humidity on ejector performance has been built. Also, a humidifier to supply humid secondary flow has been built.
2. An ejector for an 80kW class fuel cell automobile has been designed for experiment. The ejector has convergent nozzle to obtain subsonic flow inside a mixing tube. Its mixing tube is constant area type for ease of analysis and manufacture.
3. Test result shows degradation of ejector pumping up to 10% as relative humidity of secondary flow increases from 0 to 77%. Condensed water has been observed at the exit of the test ejector.

## Chapter 4.

### Modeling Results and Discussions

In this chapter, a new analytical model's prediction and experimental result will be discussed. Also, ejector characteristics, performance map and off-design characteristics will be presented.

#### 4.1 Ejector pumping and condensation

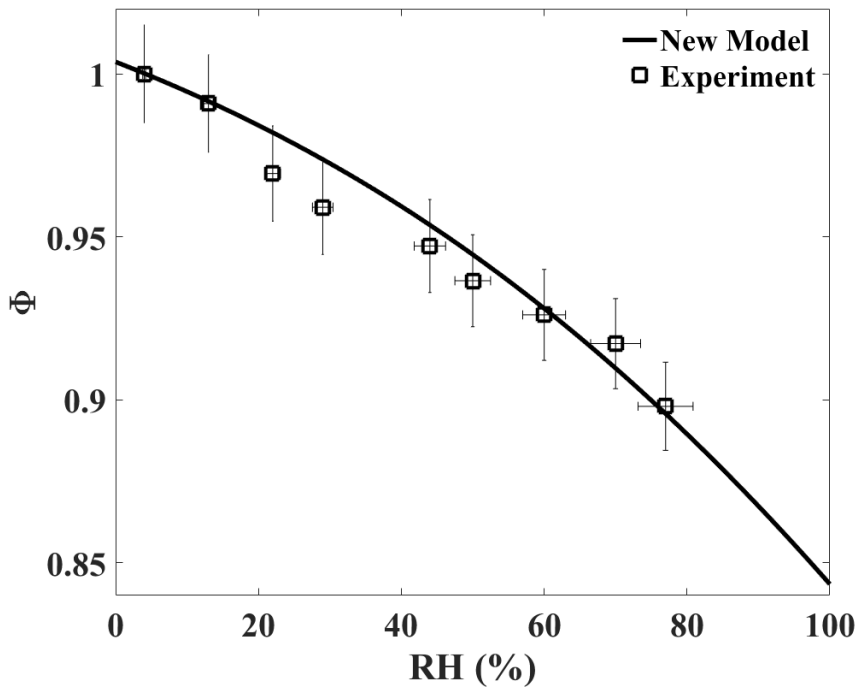


Fig. 4.1. Pumping of secondary flow vs. relative humidity.

The ejector pumping is the most important parameter of an ejector performance. Fig. 4.1 shows model's prediction of ejector pumping as well as the corresponding experimental result. The solid line is the prediction and the squares represent the experiment data. It shows degradation of pumping up to 10% as the relative humidity rises to 77% in the experiment. The model's predictions show good agreement with the experiment data. When humid secondary flow meets the primary flow at a temperature lower than the dew point of secondary flow, vapor condensation occurs. Condensation exerts heat, increasing temperature of the secondary flow in the mixing tube. The increased temperature of secondary flow decreases its density, resulting in lower entrainment. The amount of condensed water increases as the relative humidity of secondary flow increases, and the increased amount of condensed water leads to a higher temperature rise in secondary flow which further lowers density. Thus, pumping is degraded as the relative humidity of secondary flow increases. In addition, the variation of thermos-physical and transportation properties accelerates degradation of pumping.

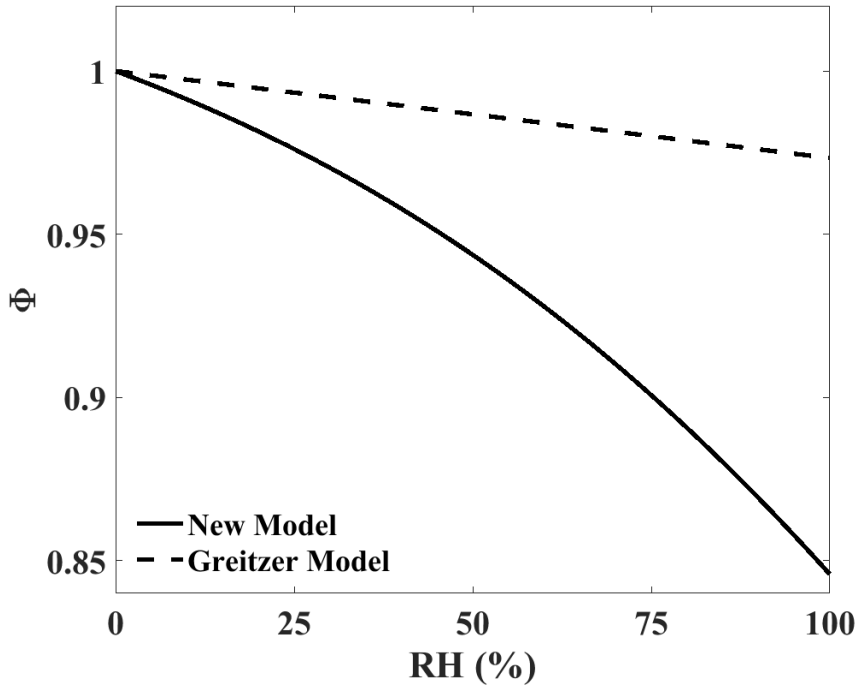


Fig. 4.2. Comparison of new model vs. Greitzer model.

The new model and Greitzer's ejector model is compared in Fig. 4.2. Greitzer's model does not have condensation terms, thus only property variations are considered. Equations used in Greitzer's model are listed in Eqs. (4.1) and (4.2).

$$\frac{\dot{m}_j \sqrt{T_{t,j}}}{A_j P_{t,j}} = \left( \frac{P_s}{P_{t,j}} \right)^{\frac{1}{k}} \left\{ \frac{2k}{R(k-1)} \left[ 1 - \left( \frac{P_s}{P_{t,j}} \right)^{\frac{k-1}{k}} \right] \right\}^{\frac{1}{2}} = f \left( \frac{P_s}{P_{t,j}} \right) \quad (4.1)$$

$$\left(\frac{\dot{m}_s}{\dot{m}_p}\right)^2 \frac{T_s}{T_p} \left[ \left(\frac{A_p}{A_s}\right)^2 + 1 \right] + 4 \left(\frac{\dot{m}_s}{\dot{m}_p}\right)^2 \sqrt{\frac{T_s}{T_p}} - 2 \frac{A_s}{A_p} = 0 \quad (4.2)$$

As shown in Eq. (4.1), the Greitzer's previous model is only affected by specific heat ratio, gas constant and density when relative humidity of a flow changes. However, the new model consists effect of condensation which shows better agreement with an experimental data.



## 4.2 Effect of secondary flow temperature on ejector performance

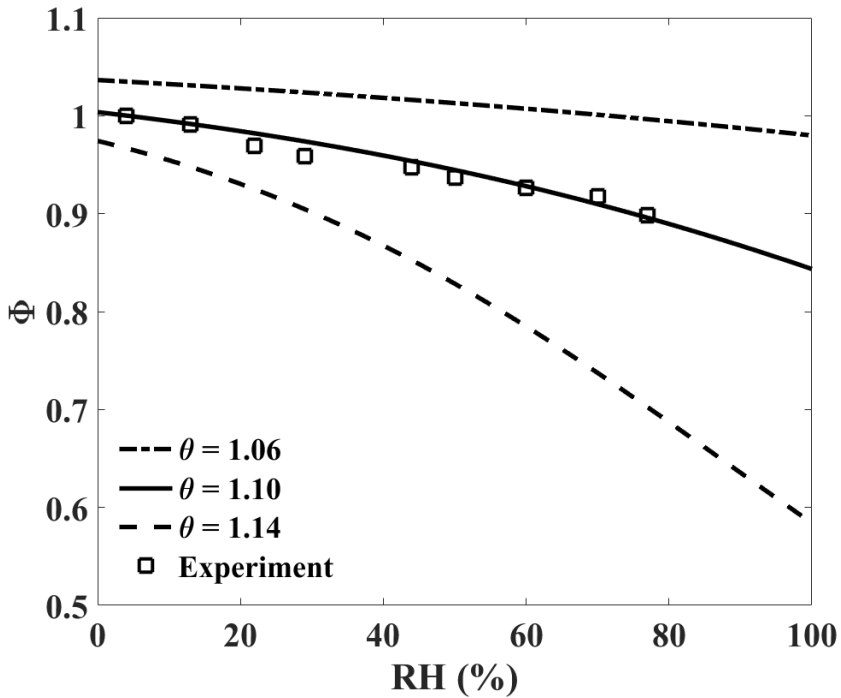


Fig. 4.3. Pumping with temperature variation ( $\theta=1.06,1.10,1.14$ ).

Fig. 4.3 shows predicted pumping for varying primary-secondary flow temperature ratios plotted vs. relative humidity. Parametric study on the variation of secondary flow temperature is important because it represents off-design operation in the fuel cell recirculation ejector. Exit temperature of the fuel cell stack varies as its power demand changes

which also changes secondary flow inlet temperature. In order to represent temperature variation, non-dimensional temperature  $\theta$  is introduced.  $\theta$  is defined as:

$$\theta = \frac{T_s}{T_p} \quad (4.1)$$

When  $\theta = 1.06$ , decrement of pumping is up to 5% as relative humidity increases from 0% to 100% while pumping decrease up to 40% when  $\theta = 1.14$ . Pumping is decreased as the relative humidity increases, but the rate of degradation is steeper at higher temperature ratios because the higher secondary flow temperature leads to higher dew point of the secondary flow. Higher temperature difference between primary flow and secondary flow's dew point increases the condensed water mass, lowering secondary flow's density and mass flow rate.

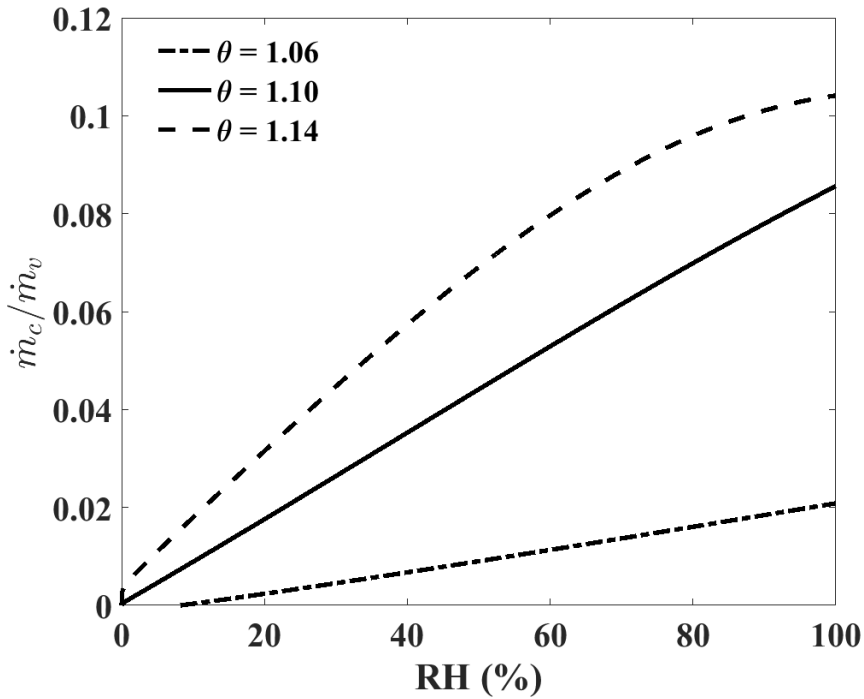


Fig. 4.4. Condensed vapor with temperature variation

( $\theta=1.06, 1.10, 1.14$ ).

Pumping decreases as the relative humidity rises, but the rate of degradation is steeper at higher temperatures because higher secondary flow temperature leads to higher dew point of secondary flow. Higher temperature difference between primary flow and secondary flow's dew point increases the condensed water mass, lowering secondary flow's density and mass flow rate. Figure 4.4 shows the predicted condensed vapor mass divided by the total vapor mass in the flow. The condensed

water mass increases as the temperature of secondary flow rises.

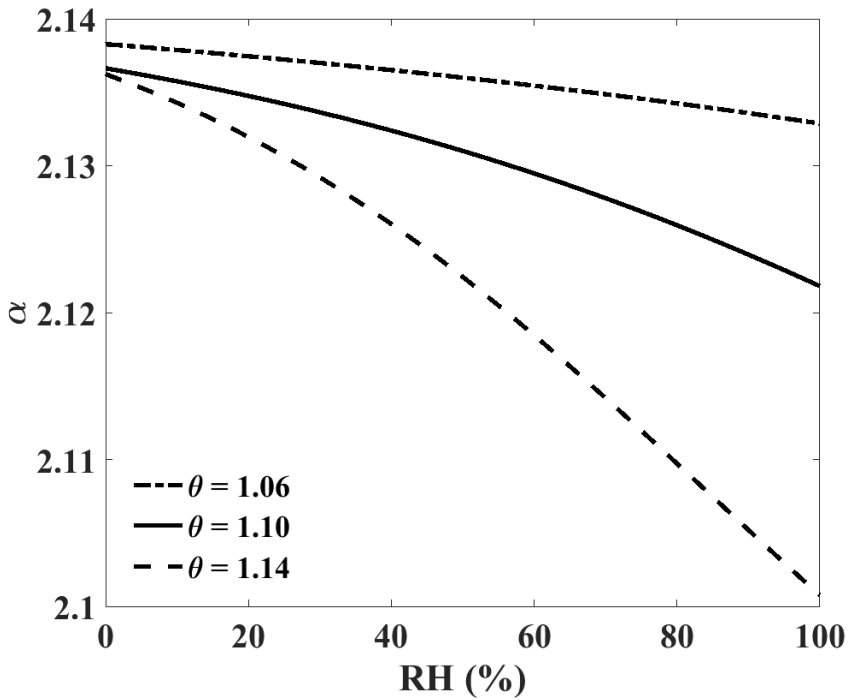


Fig. 4.5. Thrust augmentation with temperature variation

( $\theta=1.06,1.10,1.10$ ).

Fig. 4.5 shows thrust augmentation ratio with varying relative humidity and secondary flow temperature. Although a thrust augmentation has no meaning on a fuel cell recirculating ejector, it is worth noting because it can be applied to the aerospace applications such

as thrust augmentation ejector. In aerospace application, secondary flow of an ejector can be humid due to the weather condition. The thrust augmentation ratio  $\alpha$  is defined as follows:

$$\alpha = \frac{\dot{m}_e u_e}{\dot{m}_p u_p} \quad (4.2)$$

Thrust augmentation ratio shows similar trend to ejector pumping. Increased relative humidity of secondary flow decreases thrust augmentation. Also, increase of secondary flow temperature decreases thrust augmentation ratio. However, the variation of thrust augmentation ratio is up to 2%, relatively small compared to detriment of pumping.

### 4.3 Effect of pressure drop due to condensation

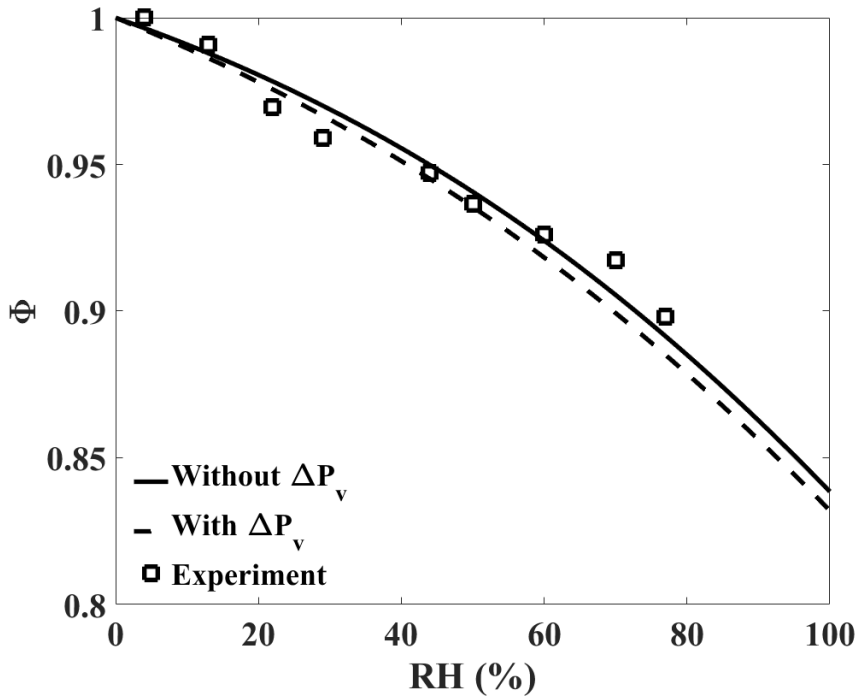


Fig. 4.6. Pumping degradation with pressure drop due to condensation.

Fig. 4.6 shows effect of pressure drop due to condensation. As previously mentioned in chapter 2, pressure inside a mixing tube decreases because vapor's partial pressure is decreased as condensation occurs. The partial pressure of condensed vapor is subtracted from a pressure inside a mixing tube. Decreased pressure inside a mixing tube leads to lowered pumping. However, the pressure drop is relatively

smaller than the effect of increased temperature due to condensation as shown in Fig. 4.6.

#### 4.4 Variation of thermo-physical properties

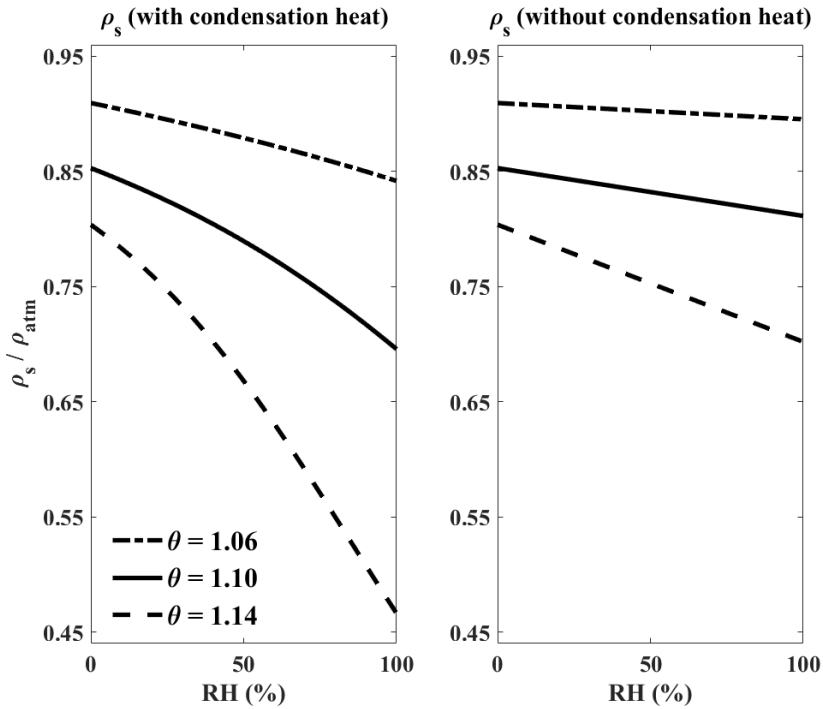


Fig. 4.7. Density variation vs. relative humidity for  $\theta = 1.06, 1.10,$  and  $1.14$ : (a) with condensation and (b) without condensation

Fig. 4.7 shows the density variation versus relative humidity for varying secondary flow temperatures. As the relative humidity rises, the density of the secondary flow is decreased. Fig. 4.7(a) shows the density variation with consideration of the heat release due to condensation. The density and consequently pumping are decreased as the relative humidity and



secondary flow temperature increase. Fig. 4.7(b) shows the density variation without consideration of the condensation heat. The density is decreased with increased relative humidity and secondary flow temperature, but the decrement is smaller than that in the Fig 4.7(a). Combined with the lowered molar mass and the exerted heat due to the condensation, density of the secondary flow is decreased more with condensation. Thus, the heat release due to condensation is an important factor degrading ejector pumping.

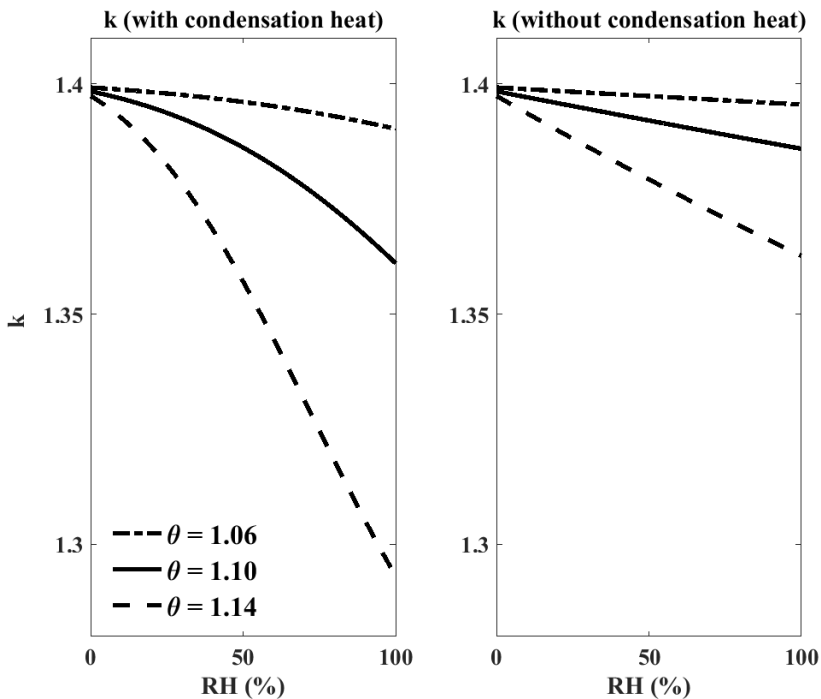


Fig. 4.8. Specific heat ratio variation vs. relative humidity for  $\theta = 1.06$ , 1.10, and 1.14: (a) with condensation and (b) without condensation.

Fig. 4.8 shows specific heat ratio variation with change of relative humidity. Fig. 4.8(a) shows specific heat ratio variation when condensation occurs. Fig. 4.8(b) shows specific heat ratio variation when there is no condensation. As figure indicates, when relative humidity increases the specific heat ratio decreases. Also, as temperature ratio increases the specific heat ratio decreases. Fig. 4.8(b) shows the specific heat ratio variation without considering condensation heat. Specific heat ratio decreases as the relative humidity and temperature ratio increases, but its decrement is smaller than the case considering condensation heat.

## 4.5 Ejector characteristics

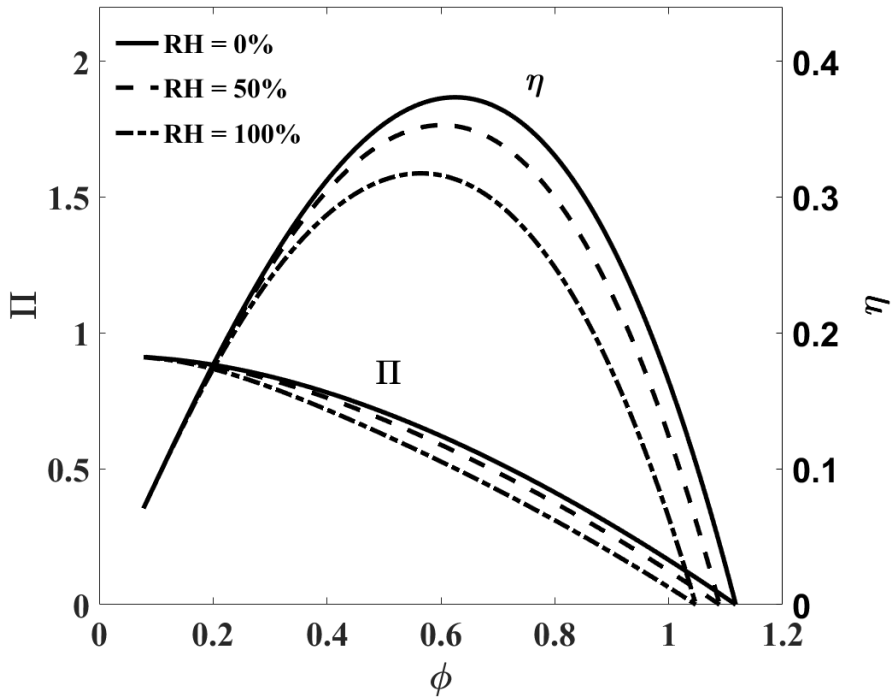


Fig. 4.9. Performance map of the ejector.

Fig. 4.9 shows performance map of the ejector designed for this study. To quantify ejector performance, the following parameters are used – pumping, pressure ratio and efficiency. [23, 24] The ejector efficiency defined in this study represents the amount of a momentum transfer between the primary and the secondary flow.

$$\phi = \frac{\dot{m}_s}{\dot{m}_p} \quad \text{ejector pumping} \quad (4.3)$$

$$\Pi = \frac{P_{t,e} - P_{t,s}}{P_{t,p} - P_{t,e}} \quad \text{pressure ratio} \quad (4.4)$$

$$\eta = \Pi \cdot \phi \quad \text{ejector efficiency} \quad (4.5)$$

As the relative humidity increases, the operating range of the ejector is narrowed by 8%. Also, the efficiency of an ejector decreases by up to 10%. The physical interpretation of the efficiency defined in this study is how much of the momentum of the primary flow has been transferred to the secondary flow. As the relative humidity increases pumping is decreased, reducing the efficiency of an ejector.

The operation map provides guideline to controlling an ejector system. In a fuel cell recirculation system, pressure ratio or mass flow rate of primary flow are controlled to match the target flow rate of fuel depending on an operating condition. The new model provides additional information when primary or secondary flow is humid. It is important because performance of an ejector degrades when flow inside an ejector is humid. The degraded flow rate can be overcome by increasing pressure ratio or mass flow rate of primary flow.

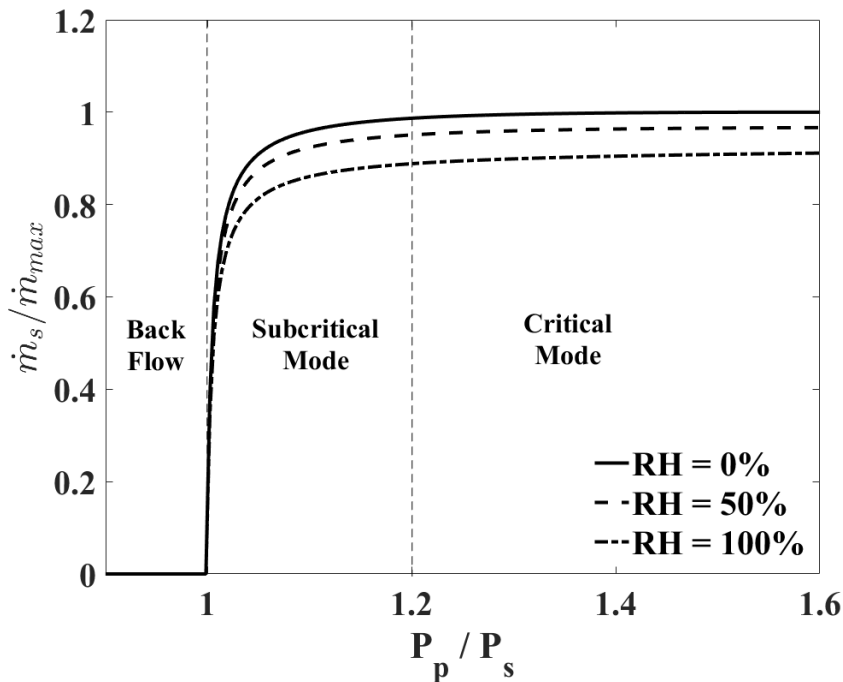


Fig. 4.10. Operational modes of an ejector.

Fig. 4.10 shows operation modes of an ejector. An ejector has three different operational modes. The backflow mode is a malfunction of an ejector where entrainment is reversed. In a subcritical mode, ejector's primary flow is choked, while secondary flow is not. At subcritical mode the pumping of an ejector changes as a pressure ratio varies. The primary flow is subsonic when an ejector operates in this mode. The critical mode has both primary and secondary flow choked, remaining constant ejector pumping. At this mode, the primary flow is sonic which is not desirable in fuel cell recirculation ejector.

As the Fig. 4.10 shows, a relative humidity affects only the pumping while critical point where ejector's operating mode shifts from subcritical to critical mode. The critical pressure ratio of an ejector can be expressed as following:

$$\pi_{critical} = \left( \frac{k_e + 1}{2} \right)^{\frac{k_e}{k_e - 1}} \quad (4.4)$$

Eq. (4.4) shows that critical pressure ratio is a function of specific heat ratio at the exit. Despite the change of specific heat ratio due to a relative humidity, it is not sensitive to relative humidity.

Understanding operating mode of an ejector is important because as pressure ratio of an ejector reaches to critical pressure ratio, the primary flow become sonic. The increased speed of flow inside an ejector can damage the fuel cell stack which is not desired in real application.

## 4.6 Conclusions

This chapter presents new analytical model's predictions. Analytical model shows pumping degradation up to 15% as relative humidity increases to 100% which is well matched to the experimental result.

Degradation in pumping performance is caused by changes in the humid air properties as well as condensation. As the relative humidity increases, the properties of humid air such as specific heat and specific heat ratio decrease, lowering pumping. Furthermore, when a dry, cold primary flow and a hot, humid air secondary flow are mixed, the heat release from condensation increases the flow temperature in the mixing tube, decreasing both density and entrainment.

Also, when temperature difference between primary and secondary flow increases, degradation of pumping is increased because condensation rate is increased. In a thrust point of view, thrust augmentation is decreased as relative humidity increases. It shows similar trend as pumping degradation, but its effect is relatively small than that of pumping.

The reduced pumping narrows the operating range of an ejector by 8% and decreases ejector efficiency by up to 10%. Main reason of reduced operating range is reduced pumping. While performance map of an

ejector is sensitive to the relative humidity, the operational modes of an ejector are not sensitive to relative humidity. Its key factor, critical pressure ratio, is a function of specific heat ratio and it is not sensitive to variation of relative humidity.



## Chapter 5.

### Summary and Conclusions

This study has been conducted to understand the effect of relative humidity on ejector performance. In this study, an ejector used as fuel recirculation pump in fuel cell automobile has been analyzed and tested. During the fuel recirculation process, unreacted hydrogen and water vapor generated by fuel cell reaction is supplied to the ejector, making secondary flow humid. Humid secondary flow can affect ejector performance such as ejector pumping and operating range. To understand effect of humidity on ejector performance, analytical model was developed. The new model has been constructed based on isentropic relation, correlation of thermo-physical properties, condensation during a mixing process, and conservation laws. The analytical model has been verified by experimental results.

New model can predict relative humidity effect on ejector performance such as ejector pumping, operating range, efficiency and operational modes. As relative humidity increases, pumping of the ejector decreases up to 15% at maximum relative humidity of 100%.

Also operating range is narrowed by 8% as relative humidity increases. Efficiency of the ejector is lowered up to 10% as relative humidity increases. However, critical pressure ratio of operating mode is not sensitive to the change of relative humidity.

Experiment has been conducted to validate the new analytical model. Relative humidity of the secondary flow has been controlled from 4% to 77% to measure pumping of an ejector. Experiment result shows degradation of pumping up to 10% when relative humidity rises from 4% to 77% which is well matched to the new analytical model.

The degradation in pumping performance is caused by changes in the humid air properties as well as condensation. As the relative humidity increases, the properties of humid air such as specific heat and specific heat ratio decrease, lowering pumping. Furthermore, when a dry, cold primary flow and a hot, humid air secondary flow are mixed, the heat release from condensation increases the flow temperature in the mixing tube, decreasing both density and entrainment.

Lowered pumping performance causes other ejector performances such as operating range and efficiency to be degraded. Operating range is narrowed as it is direct function of the ejector pumping. Efficiency of the ejector is also decreased because of lowered density and pumping.

Compared with previous analytical model of ejectors, the new model can predict effect of condensation and change of thermo-physical properties of humid working fluid in an ejector. Not only the features mentioned above, it is capable of describe ejector characteristic curves and operational modes as previously developed one-dimensional models by other researchers. Also, analysis of general ‘humid’ gas can be conducted using the new model by using proper humid gas correlations.

## References

- [1] Keenan, J. H, and Neumann, E. P., 1942, “A Simple Air Ejector,” *Journal of Applied Mechanics*, **9**, A75-A81.
- [2] Elrod, H. G, 1945, “The Theory of Ejectors”, *Journal of Applied Mechanics*, **12**, pp. A170-A174.
- [3] Eames, I. W, Aphornratana, S., and Haider, H., 1995, “A Theoretical and Experimental Study of a Small-scale Steam Jet Refrigerator,” *International Journal of Refrigeration*, **18**, pp. 378-386.
- [4] Huang, B. J., Chang, J. M., Wang, C. P., and Petrenko, V. A., 1999, “A 1-D Analysis of Ejector Performance,” *International Journal of Refrigeration*, **22**, pp. 354-364.
- [5] Presz, W. M., and Greitzer, E. M., 1988, “A Useful Similarity Principle for Jet Engine Exhaust System Performance,” 24th ASME, SAE, and ASEE Joint Propulsion Conference.
- [6] Elbel, S., 2011, “Historical and present developments of ejector refrigeration systems with emphasis on transcritical carbon dioxide air-conditioning applications”, *International Journal of Refrigeration*, **34**(7), pp. 1545-1561.
- [7] Shirey, D. B. I. I. I., 1993. “Demonstration of efficient humidity

control techniques at an art museum”, 1993 Winter Meeting of ASHRAE Transactions. Part 1, Chicago, IL, USA, 01/23-27/93, pp. 694-703.

[8] American Society of Heating, Refrigerating, and Air-conditioning Engineers (ASHRAE), 1983, “Handbook: Equipment, Chapter 13: Steam-jet refrigeration equipment”, Atlanta, GA, USA.

[9] U.S. Department of Transportation, FAA, 1993, “Basic Helicopter Handbook”, DIANE Publishing.

[10] Sherif, S. A., et al. 2000. "Analysis and modeling of a two-phase jet pump of a thermal management system for aerospace applications." International journal of mechanical sciences **42**(2) pp. 185-198.

[11] Cizungu, K., M. Groll, and Z. G. Ling., 2005. "Modelling and optimization of two-phase ejectors for cooling systems." Applied thermal engineering Vol. **25**(13) pp. 1979-1994.

[12] Marsano, F., Magistri, L., & Massardo, A. F., 2004. “Ejector performance influence on a solid oxide fuel cell anodic recirculation system.” Journal of Power Sources, **129**(2), pp.216-228.

[13] Kim, M., Sohn, Y. J., Cho, C. W., Lee, W. Y., & Kim, C. S. 2008., “Customized design for the ejector to recirculate a humidified hydrogen

fuel in a submarine PEMFC.” *Journal of Power Sources*, **176**(2), pp.529-533.

[14] Zhu, Y., & Li, Y. 2009, “New theoretical model for convergent nozzle ejector in the proton exchange membrane fuel cell system”, *Journal of Power Sources*, **191**(2), pp. 510-519.

[15] Engelbracht, M., Peters, R., Blum, L., & Stolten, D., 2015. “Comparison of a fuel-driven and steam-driven ejector in solid oxide fuel cell systems with anode off-gas recirculation: Part-load behavior”. *Journal of power sources*, 277, pp.251-260.

[16] Greitzer, E. M., Tan, C. S., & Graf, M. B., 2007, “Internal flow: concepts and applications (Vol. 3)”, Cambridge University Press.

[17] Coleman, H. W., & Steele, W. G., Experimentation, validation, and uncertainty analysis for engineers, *John Wiley & Sons*. (2009)

[18] Lin, X., and K. G. Hubbard, Uncertainties of derived dewpoint temperature and relative humidity. *Journal of applied meteorology* 43.5 (2004): 821-825.

[19] Tsilingiris, P. T., 2008. “Thermophysical and transport properties of humid air at temperature range between 0 and 100°C.” *Energy Conversion and Management* **49**, pp. 1098-1110.

[20] Greitzer, EM, Paterson, RW & Tan, CS. 1985. “An approximate substitution principle for viscous heat conducting flows” Proceedings of the Royal Society of London. A. Mathematical and Physical Sciences **401**, pp. 163-193.

[21] Nusselt., W., 1916. “Die Oberflächenkondensation des Wasserdampfes” Z. Ver. Deut. Ing. **60**, pp. 569-575.

[22] Rohsenow, W. M., 1956. “Heat Transfer and Temperature Distribution in Laminar Film Condensation.” Trans. ASME, **78** pp. 1645-1648.

[23] Meakhail, T. A., Zien, Y., Elsallak, M., & AbdelHady, S., 2008, “Experimental study of the effect of some geometric variables and number of nozzles on the performance of a subsonic air—air ejector”, Proceedings of the Institution of Mechanical Engineers, Part A: Journal of Power and Energy, **222**(8), pp. 809-818.

[24] M. Flouros, F. Cottier, M. Hirchnann, J. Kutz, and A. Jocher, Ejector scavenging of bearing chambers. A numerical and experimental investigation, *Journal of Engineering for Gas Turbines and Power*, 135(8) (2013) 081602.

[25] Carletti, M. J., Rogers, C. B., and Parekh, D. E., 1995, "Use of Streamwise Vorticity to Increase Mass Entrainment in a Cylindrical

Ejector," AIAA Journal, **33**(9) pp. 1641.

[26] McBean, S. F., and A. M. Birk., 2006, "The performance of air-air ejectors with triangular tabbed driving nozzles." ASME Turbo Expo 2006: Power for Land, Sea, and Air. American Society of Mechanical Engineers.

[27] Im, J. H., & Song, S. J., 2015, "Mixing and entrainment characteristics in circular short ejectors", Journal of Fluids Engineering, **137**(5), 051103.

[28] Chen, S. L., Yen, J. Y., and Huang, M. C., 1998, "An experimental investigation of ejector performance based upon different refrigerants", ASHRAE Transaction, **104**(2), pp. 150-160.

[29] Dong J, Pounds DA, Cheng PP, Ma HB., 2012, "An Experimental Investigation of Steam Ejector Refrigeration Systems." ASME. J. Thermal Sci. Eng. Appl. **4**(3)



국문초록

# 상대습도가 이젝터 성능에 미치는 영향에 대한 해석

이호채

서울대학교 대학원

기계항공공학부

2007-20844

이젝터는 노즐과 흡입구, 그리고 혼합챔버로 이루어진 간단한 구조의 펌프이다. 이젝터는 단순한 구조로 인해 냉동, 공조, 항공 등 여러 산업분야에 쓰인다. 이 연구에서는 수소연료 자동차에서 사용되는 연료순환용 이젝터를 다룬다. 연료전지에서는 효율을 높이기 위해 수소를 과공급하며 연료전지 출구로 반응하지 못한 수소와 반응물인 수증기가 섞여서 배출된다. 이 미반응 수소와 수증기는 연료효율 증가를 위해 이젝터를 이용해 주유동과 혼합, 재순환시키게 된다. 이때문에 이젝터의 흡입유동은 습한 상태가 된다. 작동유체의 상대습도가 변

하게 되면 유동의 특성이 변하게 되며 이는 이젝터의 성능에 영향을 미칠 수 있다. 이 연구에서는 상대습도가 이젝터의 성능에 미치는 영향을 해석적 방법으로 접근하였으며 해석적 모델의 예측과 실험 결과를 비교하였다. 실험에서는 상대습도를 증가시키면 이젝터의 펌핑이 최대 10%까지 감소하는 것을 관측하였으며 새로운 해석적 모델의 예측과 일치하였다. 이러한 현상은 건조한 주유동과 습한 흡입유동이 혼합되며 응축이 발생하고 이에 따른 잠열발생으로 유동의 온도가 증가해 밀도가 감소하는 것이 원인이다. 또한 상대습도가 증가하면 흡입유동의 밀도가 추가로 감소하여 이젝터의 흡입량을 감소시키는 원인이 된다. 이러한 흡입유동의 감소는 이젝터의 성능곡선에서 효율을 최대 10%까지 감소시키며 작동범위또한 8% 감소된다.

주제어: 이젝터 성능, 상대습도, 응축, 수소연료자동차